Distributed Control of Robotic Networks

A Mathematical Approach to Motion Coordination Algorithms

Chapter 2: Geometric models and optimization

Francesco Bullo
Jorge Cortés
Sonia Martínez

May 20, 2009

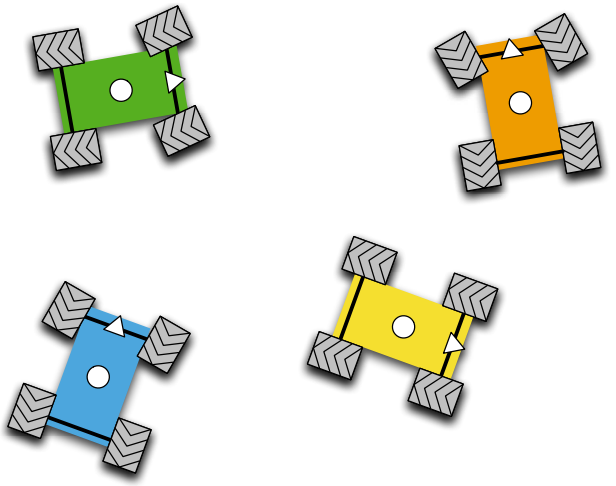

PRINCETON UNIVERSITY PRESS
PRINCETON AND OXFORD

Distributed Control of Robotic Networks, by Francesco Bullo, Jorge Cortés and Sonia Martínez, Applied Mathematics Series, Princeton University Press, 2009, ISBN 978-0-691-14195-4.

The book is available online at

http://coordinationbook.info

Contents

Chapter Two

Geometric models and optimization

This chapter presents various geometric objects and geometric optimization problems that have strong connections with motion coordination. Basic geometric notions such as polytopes, centers, partitions, and distances are ubiquitous in cooperative strategies, coordination tasks, and the interaction of robotic networks with the physical environment. The notion of Voronoi partition finds application in diverse areas such as wireless communications, signal compression, facility location, and mesh optimization. Proximity graphs provide a natural way to mathematically model the network interconnection topology resulting from the agents' sensing and/or communication capabilities. Finally, multicenter functions play the role of aggregate objective functions in geometric optimization problems. We introduce these concepts here in preparation for the later chapters.

The chapter is organized as follows. We begin by presenting basic geometric constructions. This gives way to introduce the notion of proximity graphs along with numerous examples. The next section of the chapter presents geometric optimization problems and multicenter functions, paying special attention to the characterization of their smoothness properties and critical points. We end the chapter with three sections on, respectively, bibliographic notes, proofs of the results presented in the chapter, and exercises.

2.1 BASIC GEOMETRIC NOTIONS

In this section, we gather some classical geometric constructions that will be invoked regularly throughout the book.

2.1.1 Polygons and polytopes

For $p, q \in \mathbb{R}^d$, we let $]p, q[= \{\lambda p + (1-\lambda)q \mid \lambda \in]0, 1[\}$ and $[p, q] = \{\lambda p + (1-\lambda)q \mid \lambda \in [0, 1]\}$ denote the *open segment* and *closed segment*, with extreme

points p and q, respectively. We let $H_{p,q} = \{x \in \mathbb{R}^d \mid \|x - p\|_2 \leq \|x - q\|_2\}$ denote the *closed halfspace* of $\mathbb{R}^d$ of points closer (in Euclidean distance) to p than to q. In the plane, we often refer to a halfspace as a *halfplane*.

As seen in Section 1.2, a set $S \subset \mathbb{R}^d$ is *convex* if, for any two points p, q in S, the closed segment $[p, q]$ is contained in S. The *convex hull* of a set is the smallest (with respect to the inclusion) convex set that contains it. We denote the convex hull of S by $\mathrm{co}(S)$. For $S = \{p_1, \ldots, p_n\}$ finite, the convex hull can be explicitly described as follows:

$$\mathrm{co}(S) = \big\{\lambda_1 p_1 + \cdots + \lambda_n p_n \mid \lambda_i \geq 0 \text{ and } \sum_{i=1}^{n} \lambda_i = 1\big\}.$$

Given p and q in $\mathbb{R}^d$ and a convex closed set $Q \subset \mathbb{R}^d$ with $p \in Q$ (see Figure 2.1), define the *from-to-inside* function by

$$\mathrm{fti}(p, q, Q) = \begin{cases} q, & \text{if } q \in Q, \\ [p, q] \cap \partial Q, & \text{if } q \notin Q. \end{cases}$$

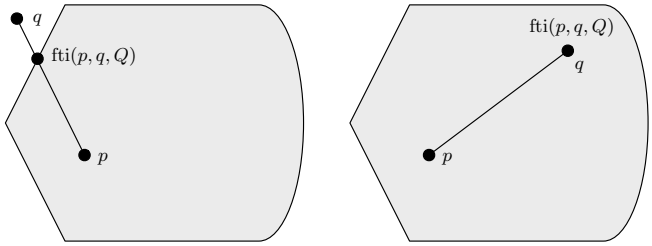

Figure 2.1 An illustration of the from-to-inside function fti.

The function fti selects the point in the closed segment $[p, q]$ which is at the same time closest to q and inside Q. Note that $\mathrm{fti}(p, q, Q)$ depends continuously on p and q.

A *polygon* is a set in $\mathbb{R}^2$ whose boundary is the union of a finite number of closed segments. A polygon is *simple* if its boundary, regarded as a curve, is not self-intersecting. We will only consider simple polygons. The closed segments composing the boundary of a polygon are called *edges*, and points resulting from the pairwise intersection between consecutive edges are called *vertices*. A convex polygon can be written as:

(i) the convex hull of its set of vertices; or

(ii) the intersection of halfplanes defined by its edges.

Two vertices whose open segment is contained in the interior of the polygon define a *diagonal*. To each vertex of a polygon we associate an *interior* and an *exterior angle*. A vertex is *strictly convex* (resp. *strictly nonconvex*) if its interior angle is strictly smaller (resp. greater) than π radians. A polygon is nonconvex if it has at least one strictly concave vertex. The *perimeter* of a polygon is the length of its boundary, that is, the sum of the lengths of its edges. A polytope is the generalization of the notion of polygon to $\mathbb{R}^d$, for $d \geq 3$. In this book, we will not consider nonconvex polytopes in dimension larger than 2. As for convex polygons, a *(convex) polytope* in $\mathbb{R}^d$ can be defined as either the convex hull of a finite set of points in $\mathbb{R}^d$ or the bounded intersection of a finite set of halfspaces. A $d-1$ *face* (or a *facet*) of a polytope is the intersection between the polytope and the boundary of a closed halfspace that defines the polytope. A $d-2$ face is a $d-2$ face of a facet of the polytope. The faces of dimensions 0, 1, and $d-1$ are called *vertices*, *edges*, and *faces*, respectively. For a convex polytope Q, we will refer to them as $\mathrm{Ve}(Q)$, $\mathrm{Ed}(Q)$, and $\mathrm{Fa}(Q)$, respectively.

2.1.2 Nonconvex geometry

In this section, we gather some basic notions on nonconvex geometry. We consider environments that include nonconvex polygons as a particular case.

We begin with some visibility notions. Given $S \subset \mathbb{R}^d$, two points $p, q \in S$ are *visible* to each other if the closed segment $[p, q]$ is contained in S. The *visibility set* $\mathrm{Vi}(p; S)$ is the set of all points in S visible from p. Given $r > 0$, the *range-limited visibility set* $\mathrm{Vi}_{\mathrm{disk}}(p; S) = \mathrm{Vi}(p; S) \cap \overline{B}(p, r)$ is the set of all points in S within a distance r and visible from p. The set S is *star-shaped* if there exists $p \in S$ such that $\mathrm{Vi}(p; S) = S$. The *kernel set* of S is comprised of all the points with this property, that is, $\mathrm{kernel}(S) = \{p \in S \mid \mathrm{Vi}(p; S) = S\}$. Trivially, any convex set is star-shaped. Given $\delta \in \mathbb{R}_{>0}$, the δ-contraction of S is the set $S_\delta = \{p \in S \mid \mathrm{dist}(p, \partial S) \geq \delta\}$. Note that if two points $p, q \in S$ are visible to each other in S_δ, then any point within distance δ of p and any point within distance δ of q are visible to each other. Figure 2.2 illustrates these visibility notions.

Next, we introduce various concavity notions. Given $S \subset \mathbb{R}^d$ connected and closed, $p \in \partial S$ is *strictly concave* if, for any $\varepsilon \in \mathbb{R}_{>0}$, there exist $q_1, q_2 \in B(p, \varepsilon) \cap \partial S$ such that $[q_1, q_2] \not\subset S$. This definition coincides with the notion of strictly concave vertex when the set S is a polygon. A *strict concavity* of S is either an isolated strictly concave point or a concave arc, that is, a connected set of strictly concave points. An *allowable environment* $S \subset \mathbb{R}^2$ is a set that satisfies the following properties: it is closed, simply connected, has a finite number of strict concavities, and its boundary can

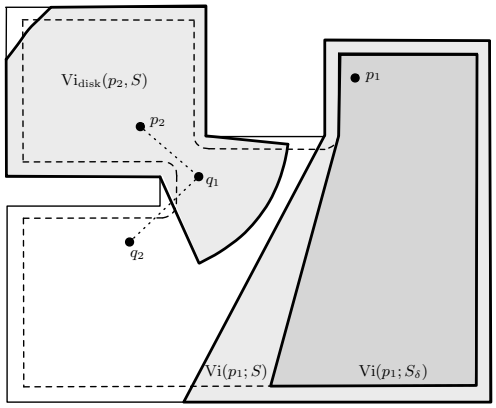

Figure 2.2 An illustration of various visibility notions. The visibility set $\mathrm{Vi}(p_1; S)$ from p_1 in S, the visibility set $\mathrm{Vi}(p_1; S_\delta)$ from p_1 in S_δ, and the range-limited visibility set $\mathrm{Vi}_{\mathrm{disk}}(p_2; S)$ from p_2 in S are depicted in light gray. The dashed curve in the interior of S corresponds to the boundary of the δ-contraction of S. The points p_2 and q_1 are visible to each other in S_δ. The points q_1 and q_2 are visible to each other in S, but they are not visible to each other in S_δ.

be described by a continuous and piecewise continuously differentiable curve which is not differentiable at most at a finite number of points. Figure 2.3 shows a sample allowable environment. Given an allowable environment S, let a point v belonging to a concave arc have the property that the boundary of S is continuously differentiable at v. The *internal tangent halfplane* $H_S(v)$ is the closed halfplane whose boundary is tangent to ∂S at v and whose interior does not contain any points of the strict concavity (see Figure 2.3).

The following result presents an interesting property of allowable environments. Its proof is left to the reader.

Lemma 2.1 (Contraction of allowable environments). *Given an allowable environment S, the δ-contraction S_δ is also allowable for sufficiently small $\delta \in \mathbb{R}_{>0}$ and does not have isolated strictly concave points. Furthermore, the boundary of S_δ is continuously differentiable at the concavities.*

Lemma 2.1 implies that the internal tangent halfplane is well-defined at any strict concavity of the δ-contraction S_δ.

A set $S \subset X$ is *relatively convex* in $X \subset \mathbb{R}^d$ if, for any two points p, q in S, the shortest curve in X that connects p and q is contained in S. Relatively convex sets in $\mathbb{R}^d$ are just convex sets. The *relative convex hull* of a set S in X is the smallest (with respect to the operation of inclusion)

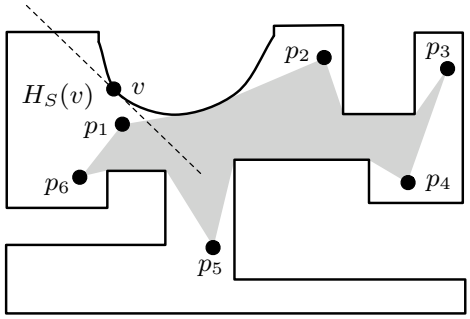

Figure 2.3 An allowable environment S. The curved portion of the boundary is a concave arc. The vertices whose interior angle is $3\pi/2$ radians are isolated strictly concave points. The relative convex hull of $\{p_1, \ldots, p_6\}$ in S is depicted in light gray. Finally, the dashed line represents the boundary of the internal tangent halfplane $H_S(v)$ tangent to ∂S at v.

relatively convex set in X that contains S (see Figure 2.3). We denote the relative convex hull of S in X by $\mathrm{rco}(S; X)$. The *(relative) perimeter* of S in X is the length of the shortest measurable closed curve contained in X that encloses S.

2.1.3 Geometric centers

Let $X = \mathbb{R}^d$, $X = \mathbb{S}^d$ or $X = \mathbb{R}^{d_1} \times \mathbb{S}^{d_2}$, $d = d_1 + d_2$. Recall our convention (cf., Section 1.1.2) that, unless otherwise noted, $\mathbb{R}^d$ is endowed with the Euclidean distance, $\mathbb{S}^d$ is endowed with the geodesic distance, and $\mathbb{R}^{d_1} \times \mathbb{S}^{d_2}$ is endowed with the Cartesian product distance $(\mathrm{dist}_2, \mathrm{dist}_g)$.

The *circumcenter* of a bounded set $S \subset X$, denoted by $\mathrm{CC}(S)$, is the center of the closed ball of minimum radius that contains S. The *circumradius* of S, denoted by $\mathrm{CR}(S)$, is the radius of this ball[1]. The circumcenter is always unique.

The computation of the circumcenter and the circumradius of a polytope $Q \subset \mathbb{R}^d$ is a strictly convex problem and, in particular, a quadratically constrained linear program in p (the center) and r (the radius). It consists of minimizing the radius r of the ball centered at p subject to the constraints that the distance between q and each of the polygon vertices is smaller than

[1]Note that the definition of circumcenter given here is in general different from the classical notion of circumcenter of a triangle, that is, the center of the circle passing through the three vertices of the triangle.

or equal to r. Formally, the problem can be expressed as

$$\begin{aligned} &\text{minimize } r\,, \\ &\text{subject to } \|q-p\|_2^2 \leq r^2, \text{ for all } q \in \mathrm{Ve}(Q). \end{aligned} \tag{2.1.1}$$

Next, we summarize some useful properties of the circumcenter in Euclidean space; see Exercise E2.1 for their proofs. In the following result, for $S \in \mathbb{F}(\mathbb{R}^d)$ with $d = 1$, we let $\mathrm{Ve}(\mathrm{co}(S))$ denote the set of extreme points of the interval $\mathrm{co}(S)$.

Lemma 2.2 (Properties of the circumcenter in Euclidean space). *Let $S = \{p_1, \ldots, p_n\} \in \mathbb{F}(\mathbb{R}^d)$ with $n \geq 2$. The following properties hold:*

(i) $\mathrm{CC}(S) \in \mathrm{co}(S) \setminus \mathrm{Ve}(\mathrm{co}(S))$*; and*

(ii) if $p \in \mathrm{co}(S) \setminus \{\mathrm{CC}(S)\}$ and $r \in \mathbb{R}_{>0}$ are such that $S \subset \overline{B}(p, r)$, then $]p, \mathrm{CC}(S)[$ has a nonempty intersection with $\overline{B}(\frac{p+q}{2}, \frac{r}{2})$ for all $q \in \mathrm{co}(S)$.

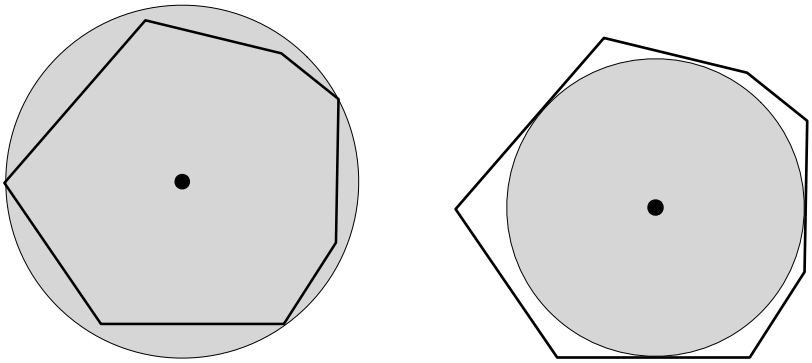

Figure 2.4 The circumcenter and circumradius (left), and incenter and inradius (right) of a convex polygon.

Given $X = \mathbb{R}^d$, $X = \mathbb{S}^d$ or $X = \mathbb{R}^{d_1} \times \mathbb{S}^{d_2}$, $d = d_1 + d_2$, the *incenter*, or *Chebyshev center* of a compact set $S \subset X$, denoted by $\mathrm{IC}(S)$, is the set containing the centers of all closed balls of maximum radius contained in S. The *inradius* of S, denoted by $\mathrm{IR}(S)$, is the common radius of any of these balls.

The computation of the incenter and the inradius of a polytope $Q \subset \mathbb{R}^d$ is a convex problem and, in particular, a linear program in p and r. It consists of maximizing the radius r of the ball centered at p subject to the constraints that the distance between p and each of the polytope facets is greater than or equal to r. Formally, the problem can be expressed as follows. For each

$f \in \mathrm{Fa}(Q)$, select a point $q_f \in Q$ belonging to f. Then, we set

$$\begin{aligned} &\text{maximize } r\,, \\ &\text{subject to } (q_f - p)\cdot \mathrm{n}_{\mathrm{out}} \geq r\,, \text{ for all } f \in \mathrm{Fa}(Q), \end{aligned} \tag{2.1.2}$$

where $\mathrm{n}_{\mathrm{out}}$ denotes the normal to the face f pointing toward the exterior of the polytope. The incenter of a polytope is not necessarily unique (consider, for instance, the case of a rectangle).

In Euclidean space, $X = \mathbb{R}^d$, we refer to a bounded measurable function $\phi : \mathbb{R}^d \to \mathbb{R}_{\geq 0}$ as a *density* on $\mathbb{R}^d$. The *(generalized) area* and the *centroid* (also called center of mass) of a bounded measurable set $S \subset \mathbb{R}^d$ with respect to ϕ, denoted by $\mathrm{A}_\phi(S)$ and $\mathrm{CM}_\phi(S)$ respectively, are given by

$$\mathrm{A}_\phi(S) = \int_S \phi(q)dq, \qquad \mathrm{CM}_\phi(S) = \frac{1}{\mathrm{A}_\phi(S)} \int_S q\phi(q)dq.$$

When the function ϕ that is being used is clear from the context, we simply refer to the area and the centroid of S. The centroid can alternatively be defined as follows. Define the *polar moment of inertia* of S about $p \in S$ by

$$\mathrm{J}_\phi(S, p) = \int_S \|q - p\|_2^2 \phi(q)dq.$$

Then, the centroid of S is precisely the point $p \in S$ that minimizes the polar moment of inertia of S about p. This can be easily seen from the Parallel Axis Theorem (Hibbeler, 2006), which states that

$$\mathrm{J}_\phi(S, p) = \mathrm{J}_\phi(S, \mathrm{CM}_\phi(S)) + \mathrm{A}_\phi(S)\|p - \mathrm{CM}_\phi(S)\|_2^2.$$

Remark 2.3 (Computation of geometric centers in the plane). The circumcenter, incenter, and centroid of a polygon can be computed in several ways. A simple procedure to compute the circumcenter consists of enumerating all pairs and triplets of vertices of the polygon, computing the centers and radiuses of the balls passing through them, and selecting the ball with the smallest radius that encloses the polygon. An alternative, more efficient, way of computing the circumcenter is to use the formulation (2.1.1). A convex quadratically constrained linear program is a particular case of a semidefinite-quadratic-linear program (SQLP). Several freely available numerical packages exist to solve SQLP problems; for example, SDPT3 (Tutuncu et al., 2003). The computation of the incenter set of a polygon can be performed via linear programming using the formulation (2.1.2). Finally, the centroid of a polygon can be computed with any numerical routine that accurately approximates the integral of a function over a planar domain. •

2.1.4 Voronoi and range-limited Voronoi partitions

A *partition* of a set S is a subdivision of S into connected subsets that are disjoint except for their boundary. Formally, a partition of S is a collection of closed connected sets $\{W_1, \ldots, W_m\} \subset \mathbb{P}(S)$ that verify

$$S = \cup_{i=1}^m W_i \quad \text{and} \quad \operatorname{int}(W_j) \cap \operatorname{int}(W_k) = \emptyset,$$

for $j, k \in \{1, \ldots, m\}$.

Definition 2.4 (Voronoi partition). Given a distance function $\operatorname{dist} : X \times X \to \mathbb{R}_{\geq 0}$, a set $S \subset X$ and n distinct points $\mathcal{P} = \{p_1, \ldots, p_n\}$ in S, the *Voronoi partition* of S generated by $\mathcal{P}$ is the collection of sets $\mathcal{V}(\mathcal{P}) = \{V_1(\mathcal{P}), \ldots, V_n(\mathcal{P})\} \subset \mathbb{P}(S)$ defined by, for each $i \in \{1, \ldots, n\}$,

$$V_i(\mathcal{P}) = \{q \in S \mid \operatorname{dist}(q, p_i) \leq \operatorname{dist}(q, p_j), \text{ for all } p_j \in \mathcal{P} \setminus \{p_i\}\}. \qquad \bullet$$

In other words, $V_i(\mathcal{P})$ is the set of the points of S that are closer to p_i than to any of the other points in $\mathcal{P}$. We refer to $V_i(\mathcal{P})$ as the *Voronoi cell* of p_i. Unless explicitly noted otherwise, we compute the Voronoi partition according to the following conventions:

- for $X = \mathbb{R}^d$, with respect to the Euclidean distance;
- for $X = \mathbb{S}^d$, with respect to the geodesic distance; and
- for $X = \mathbb{R}^{d_1} \times \mathbb{S}^{d_2}$, $d_1 + d_2 = d$, with respect to the Cartesian product distance determined by dist_2 on $\mathbb{R}^{d_1}$ and dist_g on $\mathbb{S}^{d_2}$.

Figure 2.5 shows an example of the Voronoi partition of the circle generated by five points. In the Euclidean case, the Voronoi cell of p_i is equal to the intersection of half-spaces determined by p_i and the other locations in $\mathcal{P}$, and as such it is a convex polytope. The left plot in Figure 2.6 shows an example of the Voronoi partition of a convex polygon generated by 40 points.

Definition 2.5 (r-limited Voronoi partition). Given a distance function $\operatorname{dist} : X \times X \to \mathbb{R}_{\geq 0}$, a set $S \subset X$, n distinct points $\mathcal{P} = \{p_1, \ldots, p_n\}$ in S, and a positive real number $r \in \mathbb{R}_{>0}$, the *r-limited Voronoi partition* inside S generated by $\mathcal{P}$ is the collection of sets $\mathcal{V}_r(\mathcal{P}) = \{V_{1,r}(\mathcal{P}), \ldots, V_{n,r}(\mathcal{P})\} \subset \mathbb{P}(S)$ defined by

$$V_{i,r}(\mathcal{P}) = V_i(\mathcal{P}) \cap \overline{B}(p_i, r), \quad i \in \{1, \ldots, n\}. \qquad \bullet$$

Note that the r-limited Voronoi partition inside S is precisely the Voronoi partition of the set $\cup_{i=1}^n \overline{B}(p_i, r) \cap S$. We will refer to $V_{i,r}(\mathcal{P})$ as the *r-limited*

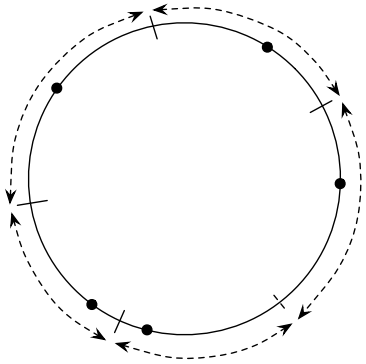

Figure 2.5 Voronoi partition of the circle generated by five points. The dashed segments correspond to the Voronoi cells of each individual point.

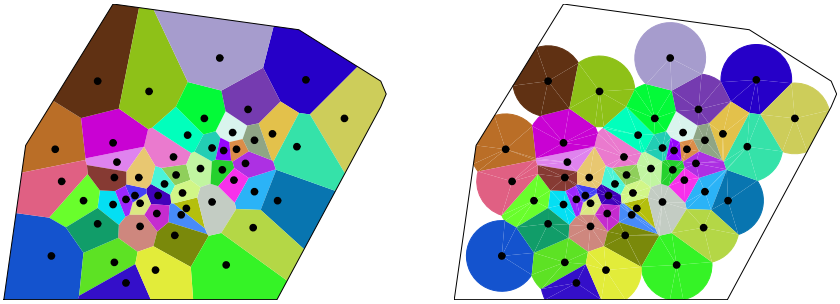

Figure 2.6 Voronoi partition of a convex polygon (left) and r-limited Voronoi partition inside a convex polygon (right) generated by 40 points.

Voronoi cell of p_i. The right-hand plot in Figure 2.6 shows an example of the r-limited Voronoi partition inside a convex polygon generated by 40 points.

Let $X = \mathbb{R}^d$, $X = \mathbb{S}^d$ or $X = \mathbb{R}^{d_1} \times \mathbb{S}^{d_2}$, $d = d_1 + d_2$. Given a density ϕ on X, a set of n distinct points $\mathcal{P} = \{p_1, \ldots, p_n\}$ in $S \subset X$ is:

(i) A *centroidal Voronoi configuration* if each point is the centroid of its own Voronoi cell, that is, $p_i = \mathrm{CM}_\phi(V_i(\mathcal{P}))$.

(ii) An *r-limited centroidal Voronoi configuration*, for $r \in \mathbb{R}_{>0}$, if each point is the centroid of its own r-limited Voronoi cell, that is, $p_i = \mathrm{CM}_\phi(V_{i,r}(\mathcal{P}))$. If $r \geq \mathrm{diam}(S)$, then an r-limited centroidal Voronoi configuration is a centroidal Voronoi configuration.

(iii) A *circumcenter Voronoi configuration* if each point is the circumcenter of its own Voronoi cell, that is, $p_i = \mathrm{CC}(V_i(\mathcal{P}))$.

(iv) An *incenter Voronoi configuration* if each point is an incenter of its own Voronoi cell, that is, $p_i \in \mathrm{IC}(V_i(\mathcal{P}))$.

Figure 2.7 illustrates of the various notions of center Voronoi configurations.

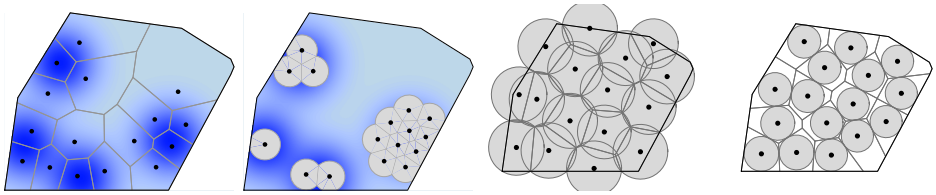

Figure 2.7 From left to right, centroidal, r-limited centroidal, circumcenter, and incenter Voronoi configurations composed by 16 points in a convex polygon. Darker blue-colored areas correspond to higher values of the density ϕ.

2.2 PROXIMITY GRAPHS

Roughly speaking, a proximity graph is a graph whose vertex set is a set of distinct points and whose edge set is a function of the relative locations of the point set. Proximity graphs appear in computational geometry. In this section, we study this important notion in detail following the presentation by Cortés et al. (2005).

Definition 2.6 (Proximity graph). Assume that X is a d-dimensional space chosen among $\mathbb{R}^d$, $\mathbb{S}^d$, and the Cartesian products $\mathbb{R}^{d_1} \times \mathbb{S}^{d_2}$, for some $d_1 + d_2 = d$. For a set $S \subset X$, let $\mathbb{G}(S)$ be the set of all undirected graphs whose vertex set is an element of $\mathbb{F}(S)$. A *proximity graph* $\mathcal{G} : \mathbb{F}(S) \to \mathbb{G}(S)$ associates to a set of distinct points $\mathcal{P} = \{p_1, \ldots, p_n\} \subset S$ an undirected graph with vertex set $\mathcal{P}$ and whose edge set is given by $\mathcal{E}_\mathcal{G}(\mathcal{P}) \subseteq \{(p, q) \in \mathcal{P} \times \mathcal{P} \mid p \neq q\}$. •

Note that in a proximity graph a point cannot be its own neighbor. From this definition, we observe that the distinguishing feature of proximity graphs is that their edge sets change with the location of their vertices. It is also possible to define proximity graphs that associate to each point set a digraph, but we will not consider them here.

Examples of proximity graphs on X, where we recall that $\mathrm{dist} = \mathrm{dist}_2$ if $X = \mathbb{R}^d$, $\mathrm{dist} = \mathrm{dist}_g$ if $X = \mathbb{S}^d$, and $\mathrm{dist} = (\mathrm{dist}_2, \mathrm{dist}_g)$ if $X = \mathbb{R}^{d_1} \times \mathbb{S}^{d_2}$, include the following:

(i) The *complete graph* $\mathcal{G}_{\mathrm{cmplt}}$ where any two points are neighbors. When convenient, we may view the complete graph as weighted by assigning the weight $\mathrm{dist}(p_i, p_j)$ to the edge $(p_i, p_j) \in \mathcal{E}_{\mathcal{G}_{\mathrm{cmplt}}}(\mathcal{P})$.

(ii) The *r-disk graph* $\mathcal{G}_{\mathrm{disk}}(r)$, for $r \in \mathbb{R}_{>0}$, where two points are neigh-

bors if they are located within a distance r, that is, $(p_i, p_j) \in \mathcal{E}_{\mathcal{G}_{\text{disk}}(r)}(\mathcal{P})$ if $\text{dist}(p_i, p_j) \leq r$.

(iii) The *Delaunay graph* $\mathcal{G}_{\text{D}}$, where two points are neighbors if their corresponding Voronoi cells intersect, that is, $(p_i, p_j) \in \mathcal{E}_{\mathcal{G}_{\text{D}}}(\mathcal{P})$ if $V_i(\mathcal{P}) \cap V_j(\mathcal{P}) \neq \emptyset$.

(iv) The *r-limited Delaunay graph* $\mathcal{G}_{\text{LD}}(r)$, for $r \in \mathbb{R}_{>0}$, where two points are neighbors if their corresponding $\frac{r}{2}$-limited Voronoi cells intersect, that is, $(p_i, p_j) \in \mathcal{E}_{\mathcal{G}_{\text{LD}}(r)}(\mathcal{P})$ if $V_{i,\frac{r}{2}}(\mathcal{P}) \cap V_{j,\frac{r}{2}}(\mathcal{P}) \neq \emptyset$.

(v) The *relative neighborhood graph* $\mathcal{G}_{\text{RN}}$, where two points are neighbors if their associated open lune (cf. Section 1.1.2) does not contain any point in $\mathcal{P}$, that is, $(p_i, p_j) \in \mathcal{E}_{\mathcal{G}_{\text{RN}}}(\mathcal{P})$ if, for all $p_k \in \mathcal{P}$, $k \notin \{i, j\}$

$$p_k \notin B(p_i, \text{dist}(p_i, p_j)) \cap B(p_j, \text{dist}(p_i, p_j)).$$

Figure 2.8 shows examples of these proximity graphs in the plane.

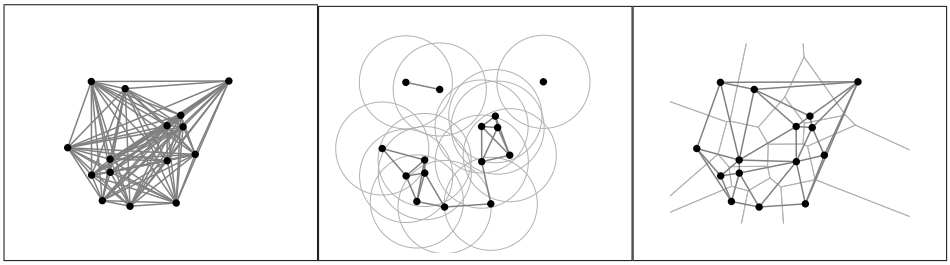

(a) $\mathcal{G}_{\text{cmplt}}$ (b) $\mathcal{G}_{\text{disk}}(r)$ (c) $\mathcal{G}_{\text{D}}$

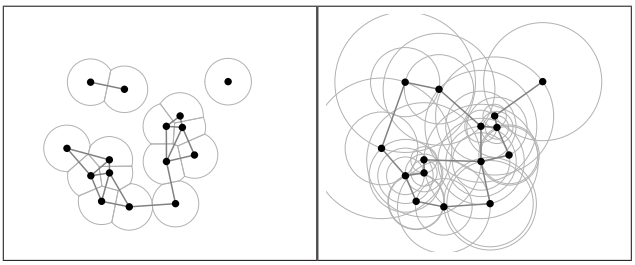

(d) $\mathcal{G}_{\text{LD}}(r)$ (e) $\mathcal{G}_{\text{RN}}$

Figure 2.8 Proximity graphs in $\mathbb{R}^2$. From left to right, in the first row, complete, r-disk, and Delaunay, and in the second row, r-limited Delaunay and relative neighborhood for a set of 15 points. When appropriate, the geometric objects determining the edge relationship are plotted in lighter gray.

Additional examples of proximity graphs in the Euclidean space include the following:

(vi) The *Gabriel graph* $\mathcal{G}_{\mathrm{G}}$, where two points are neighbors if the ball centered at their midpoint and passing through both of them does not contain any point in $\mathcal{P}$, that is, $(p_i, p_j) \in \mathcal{E}_{\mathcal{G}_{\mathrm{G}}}(\mathcal{P})$ if $p_k \notin B\big(\frac{p_i+p_j}{2}, \frac{\mathrm{dist}(p_i,p_j)}{2}\big)$ for all $p_k \in \mathcal{P}$.

(vii) The *r-∞-disk graph* $\mathcal{G}_{\infty\text{-disk}}(r)$, for $r \in \mathbb{R}_{>0}$, where two points are neighbors if they are located within L^∞-distance r, that is, $(p_i, p_j) \in \mathcal{E}_{\mathcal{G}_{\infty\text{-disk}}(r)}(\mathcal{P})$ if $\mathrm{dist}_\infty(p_i, p_j) \leq r$.

(viii) The *Euclidean minimum spanning tree* of a proximity graph $\mathcal{G}$, denoted by $\mathcal{G}_{\mathrm{EMST},\mathcal{G}}$, that assigns to each $\mathcal{P}$ a minimum-weight spanning tree (cf., Section 1.4.4.4) of $\mathcal{G}(\mathcal{P})$ with weighted adjacency matrix $a_{ij} = \|p_i - p_j\|_2$, for $(p_i, p_j) \in \mathcal{E}_{\mathcal{G}}(\mathcal{P})$. If $\mathcal{G}(\mathcal{P})$ is not connected, then $\mathcal{G}_{\mathrm{EMST},\mathcal{G}}(\mathcal{P})$ is the union of Euclidean minimum spanning trees of its connected components. When $\mathcal{G}$ is the complete graph, we simply denote the Euclidean minimum spanning tree by $\mathcal{G}_{\mathrm{EMST}}$.

(ix) the *visibility graph* $\mathcal{G}_{\mathrm{vis},Q}$ in an allowable environment Q in $\mathbb{R}^2$, where two points are neighbors if they are visible to each other, that is, $(p_i, p_j) \in \mathcal{E}_{\mathcal{G}_{\mathrm{vis},Q}}(\mathcal{P})$ if the closed segment $[p_i, p_j]$ from p_i to p_j is contained in Q.

(x) The *range-limited visibility graph* $\mathcal{G}_{\text{vis-disk},Q}$ in an allowable environment Q in $\mathbb{R}^2$, where two points are neighbors if they are visible to each other and their distance is no more than r, that is, $(p_i, p_j) \in \mathcal{E}_{\mathcal{G}_{\text{vis-disk},Q}}(\mathcal{P})$ if $(p_i, p_j) \in \mathcal{E}_{\mathcal{G}_{\mathrm{vis},Q}}(\mathcal{P})$ and $(p_i, p_j) \in \mathcal{E}_{\mathcal{G}_{\mathrm{disk}(r)}}(\mathcal{P})$.

Figure 2.9 shows examples of these proximity graphs in the plane; Figure 2.10 shows examples of these proximity graphs in a planar nonconvex environment; and Figure 2.11 shows example graphs in three-dimensions.

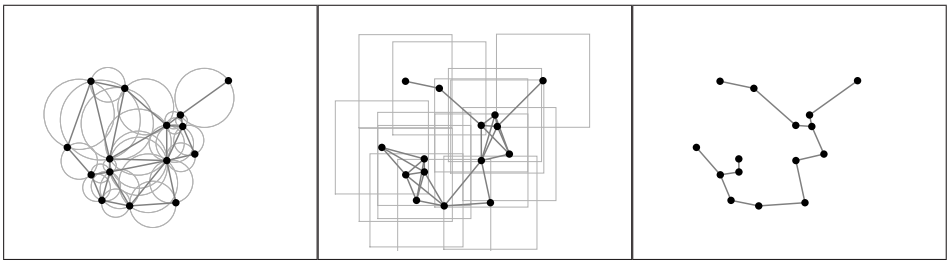

(a) $\mathcal{G}_{\mathrm{G}}$ (b) $\mathcal{G}_{\infty\text{-disk}}(r)$ (c) $\mathcal{G}_{\mathrm{EMST}}$

Figure 2.9 Proximity graphs in $\mathbb{R}^2$. From left to right, Gabriel graph, r-∞-disk graph, and Euclidean minimum spanning tree for 15 points. In two images, the geometric objects determining the edge relationship are plotted in light gray.

As for standard graphs, let us alternatively describe the edge set by means of the sets of neighbors of the individual graph vertices. To each proximity

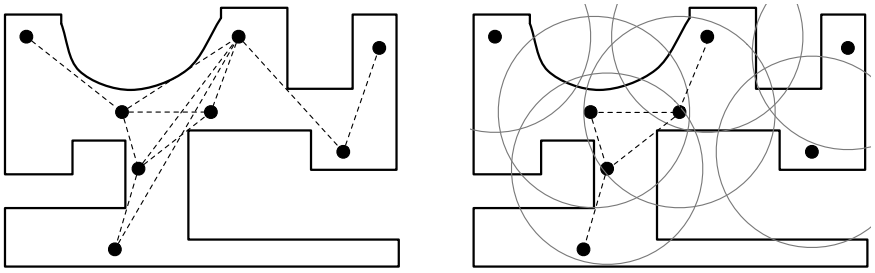

(a) $\mathcal{G}_{\text{vis},Q}$ (b) $\mathcal{G}_{\text{vis-disk},Q}$

Figure 2.10 The visibility and range-limited visibility graphs for 8 agents in an allowable environment. The geometric objects determining the edge relationship are plotted in light gray.

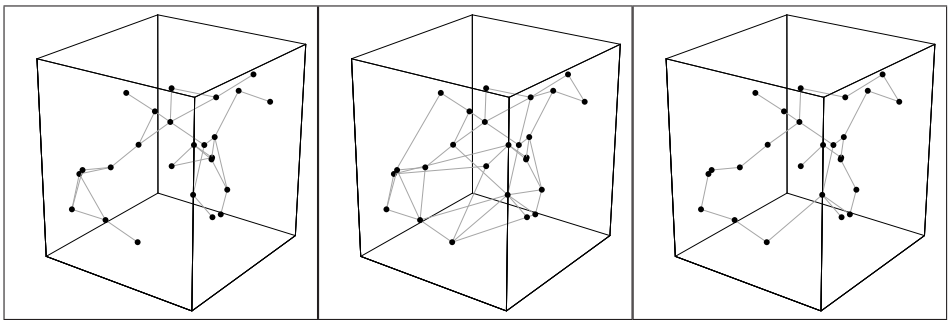

(a) $\mathcal{G}_{\text{disk}}(r)$ (b) $\mathcal{G}_{\text{G}}$ (c) $\mathcal{G}_{\text{RN}}$

Figure 2.11 Proximity graphs in $\mathbb{R}^3$. From left to right, r-disk, relative neighborhood, and Gabriel graphs for a set of 25 points.

graph $\mathcal{G}$, each $p \in X$ and each $\mathcal{P} = \{p_1, \ldots, p_n\} \in \mathbb{F}(X)$, we associate the *set of neighbors* map $\mathcal{N}_{\mathcal{G}} : X \times \mathbb{F}(X) \to \mathbb{F}(X)$ defined by

$$\mathcal{N}_{\mathcal{G}}(p, \mathcal{P}) = \{q \in \mathcal{P} \mid (p, q) \in \mathcal{E}_{\mathcal{G}}(\mathcal{P} \cup \{p\})\}.$$

Typically, p is a point in $\mathcal{P}$, but the definition is well-posed for any $p \in X$. Under the assumption that $\mathcal{P}$ does not contain repeated elements, the definition will not lead to counterintuitive interpretations later. Given $p \in X$, it is convenient to define the map $\mathcal{N}_{\mathcal{G},p} : \mathbb{F}(X) \to \mathbb{F}(X)$ by $\mathcal{N}_{\mathcal{G},p}(\mathcal{P}) = \mathcal{N}_{\mathcal{G}}(p, \mathcal{P})$.

A proximity graph $\mathcal{G}_1$ is a *subgraph* of a proximity graph $\mathcal{G}_2$, denoted $\mathcal{G}_1 \subset \mathcal{G}_2$, if $\mathcal{G}_1(\mathcal{P})$ is a subgraph of $\mathcal{G}_2(\mathcal{P})$ for all $\mathcal{P} \in \mathbb{F}(X)$. The following result, whose proof is given in Section 2.5.1, summarizes the subgraph relationships in the Euclidean case among the various proximity graphs introduced above.

Theorem 2.7 (Subgraph relationships among some standard prox-

imity graphs on $\mathbb{R}^d$). *For $r \in \mathbb{R}_{>0}$, the following statements hold:*

(i) $\mathcal{G}_{\mathrm{EMST}} \subset \mathcal{G}_{\mathrm{RN}} \subset \mathcal{G}_{\mathrm{G}} \subset \mathcal{G}_{\mathrm{D}}$*; and*

(ii) $\mathcal{G}_{\mathrm{G}} \cap \mathcal{G}_{\mathrm{disk}}(r) \subset \mathcal{G}_{\mathrm{LD}}(r) \subset \mathcal{G}_{\mathrm{D}} \cap \mathcal{G}_{\mathrm{disk}}(r)$.

Note that the inclusion $\mathcal{G}_{\mathrm{LD}}(r) \subset \mathcal{G}_{\mathrm{D}} \cap \mathcal{G}_{\mathrm{disk}}(r)$ is in general strict; this counterintuitive fact is discussed in Exercise E2.3. Additionally, since $\mathcal{G}_{\mathrm{EMST}}$ is by definition connected, Theorem 2.7(i) implies that $\mathcal{G}_{\mathrm{RN}}$, $\mathcal{G}_{\mathrm{G}}$, and $\mathcal{G}_{\mathrm{D}}$ are connected. The connectivity properties of $\mathcal{G}_{\mathrm{disk}}(r)$ are characterized in the following result.

Theorem 2.8 (Connectivity properties of some standard proximity graphs on $\mathbb{R}^d$). *For $r \in \mathbb{R}_{>0}$, the following statements hold:*

(i) $\mathcal{G}_{\mathrm{EMST}} \subset \mathcal{G}_{\mathrm{disk}}(r)$ *if and only if* $\mathcal{G}_{\mathrm{disk}}(r)$ *is connected; and*

(ii) $\mathcal{G}_{\mathrm{EMST}} \cap \mathcal{G}_{\mathrm{disk}}(r)$, $\mathcal{G}_{\mathrm{RN}} \cap \mathcal{G}_{\mathrm{disk}}(r)$, $\mathcal{G}_{\mathrm{G}} \cap \mathcal{G}_{\mathrm{disk}}(r)$ *and* $\mathcal{G}_{\mathrm{LD}}(r)$ *have the same connected components as* $\mathcal{G}_{\mathrm{disk}}(r)$ *(i.e., for all point sets* $\mathcal{P} \in \mathbb{F}(\mathbb{R}^d)$*, all graphs have the same number of connected components consisting of the same vertices).*

The proof of this theorem is given in Section 2.5.1. Note that in Theorem 2.8, fact (ii) implies (i).

2.2.1 Spatially distributed proximity graphs

We now consider the following loosely stated question: When does a given proximity graph encode sufficient information to compute another proximity graph? For instance, if a node knows the position of its neighbors in the complete graph (i.e., of every other node in the graph), then it is clear that the node can compute its neighbors with respect to any proximity graph. Let us formalize this idea. A proximity graph $\mathcal{G}_1$ is *spatially distributed over* a proximity graph $\mathcal{G}_2$ if, for all $p \in \mathcal{P}$,

$$\mathcal{N}_{\mathcal{G}_1,p}(\mathcal{P}) = \mathcal{N}_{\mathcal{G}_1,p}\big(\mathcal{N}_{\mathcal{G}_2,p}(\mathcal{P})\big),$$

that is, any node informed about the location of its neighbors with respect to $\mathcal{G}_2$ can compute its set of neighbors with respect to $\mathcal{G}_1$.

Clearly, any proximity graph is spatially distributed over the complete graph. It is straightforward to deduce that if $\mathcal{G}_1$ is spatially distributed over $\mathcal{G}_2$, then $\mathcal{G}_1$ is a subgraph of $\mathcal{G}_2$. The converse is in general not true. For instance, $\mathcal{G}_{\mathrm{D}} \cap \mathcal{G}_{\mathrm{disk}}(r)$ is a subgraph of $\mathcal{G}_{\mathrm{disk}}(r)$, but $\mathcal{G}_{\mathrm{D}} \cap \mathcal{G}_{\mathrm{disk}}(r)$ is not spatially distributed over $\mathcal{G}_{\mathrm{disk}}(r)$; see Exercise E2.4.

The following result identifies proximity graphs which are spatially distributed over $\mathcal{G}_{\text{disk}}(r)$.

Proposition 2.9 (Spatially distributed graphs over the disk graph). *The proximity graphs $\mathcal{G}_{\text{RN}} \cap \mathcal{G}_{\text{disk}}(r)$, $\mathcal{G}_{\text{G}} \cap \mathcal{G}_{\text{disk}}(r)$, and $\mathcal{G}_{\text{LD}}(r)$ are spatially distributed over $\mathcal{G}_{\text{disk}}(r)$.*

Remark 2.10 (Computation of the Delaunay graph over the r-disk graph). In general, for a fixed $r \in \mathbb{R}_{>0}$, $\mathcal{G}_{\text{D}}$ is not spatially distributed over $\mathcal{G}_{\text{disk}}(r)$. However, for a given $\mathcal{P} \in \mathbb{F}(X)$, it is always possible find r such that $\mathcal{G}_{\text{D}}(P)$ is spatially distributed over $\mathcal{G}_{\text{disk}}(r)(\mathcal{P})$. This is a consequence of the following observations. Given $\mathcal{P} \in \mathbb{F}(X)$, define the convex sets

$$W(p_i, r) = \overline{B}(p_i, r) \cap \big(\cap_{\|p_i - p_j\| \leq r} H_{p_i, p_j} \big), \quad i \in \{1, \dots, n\},$$

where we recall that $H_{p,x}$ is the half-space of points q in $\mathbb{R}^d$ with the property that $\|q - p\|_2 \leq \|q - x\|_2$. Note that the intersection $\overline{B}(p_i, r) \cap V_i$ is a subset of $W(p_i, r)$. Provided that r is twice as large as the maximum distance between p_i and the vertices of $W(p_i, r)$, then all Delaunay neighbors of p_i are within distance r from p_i. Equivalently, the half-space $H_{p_i,p}$ determined by p_i and a point p outside $\overline{B}(p_i, r)$ does not intersect $W(p_i, r)$. Therefore, the equality $V_i = W(p_i, r)$ holds. For node $i \in \{1, \dots, n\}$, the minimum adequate radius is then

$$r_{i,\min} = 2 \max\{\|p_i - q\|_2 \mid q \in W(p_i, r_{i,\min})\}.$$

The minimum adequate radius across the overall network is then $r_{\min} = \max_{i \in \{1,\dots,n\}} r_{i,\min}$. The algorithm presented in Cortés et al. (2004) builds on these observations to compute the Voronoi partition of a bounded set generated by a pointset in a distributed way. •

2.2.2 The locally cliqueless graph of a proximity graph

Given a proximity graph, it is sometimes useful to construct another proximity graph that has fewer edges and the same number of connected components. This is certainly the case when optimizing multi-agent cost functions in which the proximity graph edges describe pairwise constraints between agents. Additionally, the construction of the new proximity graph should be spatially distributed over the original proximity graph. Here, we present the notion of locally cliqueless graph of a proximity graph.

Let $\mathcal{G}$ be a proximity graph in the Euclidean space. The *locally cliqueless graph $\mathcal{G}_{\text{lc},\mathcal{G}}$ of $\mathcal{G}$* is the proximity graph defined by: $(p_i, p_j) \in \mathcal{E}_{\mathcal{G}_{\text{lc},\mathcal{G}}}(\mathcal{P})$ if

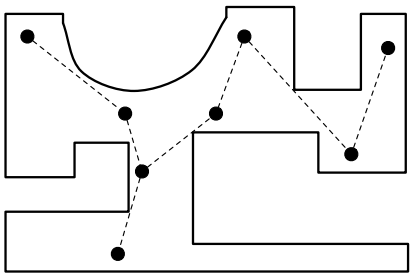

Figure 2.12 Locally cliqueless graph $\mathcal{G}_{\mathrm{lc},\mathcal{G}_{\mathrm{vis},Q}}$ of the visibility graph $\mathcal{G}_{\mathrm{vis},Q}$ for the node configuration shown in Figure 2.9(d).

$(p_i, p_j) \in \mathcal{E}_{\mathcal{G}}(\mathcal{P})$ and

$$(p_i, p_j) \in \mathcal{E}_{\mathcal{G}_{\mathrm{EMST}}}(\mathcal{P}'),$$

for any maximal clique $\mathcal{P}'$ of (p_i, p_j) in $\mathcal{G}$. Figure 2.12 shows an illustration of this notion. The properties of this construction are summarized in the following result; for the proof, see Ganguli et al. (2009).

Theorem 2.11 (Properties of the locally cliqueless graph). *Let $\mathcal{G}$ be a proximity graph in the Euclidean space. Then, the following statements hold:*

(i) $\mathcal{G}_{\mathrm{EMST},\mathcal{G}} \subseteq \mathcal{G}_{\mathrm{lc},\mathcal{G}} \subseteq \mathcal{G}$*;*

(ii) $\mathcal{G}_{\mathrm{lc},\mathcal{G}}$ *has the same connected components as* $\mathcal{G}$*; and*

(iii) for $\mathcal{G} = \mathcal{G}_{\mathrm{disk}}(r)$*,* $\mathcal{G}_{\mathrm{vis},Q}$*, and* $\mathcal{G}_{\text{vis-disk},Q}$*, where* $r \in \mathbb{R}_{>0}$ *and* Q *is an allowable environment,* $\mathcal{G}_{\mathrm{lc},\mathcal{G}}$ *is spatially distributed over* $\mathcal{G}$*.*

In general, the inclusions in Theorem 2.11(i) are strict.

2.2.3 Proximity graphs over tuples of points

The notion of proximity graph is defined for sets of distinct points $\mathcal{P} = \{p_1, \ldots, p_n\}$. However, we will be interested in considering tuples of elements of X of the form $P = (p_1, \ldots, p_n)$, where p_i corresponds to the position of an agent i of a robotic network. In principle, note that the tuple P might contain coincident points. In order to reconcile this mismatch between sets and tuples, we will do the following.

Let $i_{\mathbb{F}} : X^n \to \mathbb{F}(X)$ be the natural immersion of X^n into $\mathbb{F}(X)$, that is, $i_{\mathbb{F}}(P)$ is the point set that contains only the distinct points in $P = (p_1, \ldots, p_n)$. Note that $i_{\mathbb{F}}$ is invariant under permutations of its arguments

and that the cardinality of $i_{\mathbb{F}}(p_1, \ldots, p_n)$ is in general less than or equal to n. In what follows, $\mathcal{P} = i_{\mathbb{F}}(P)$ will always denote the point set associated to $P \in X^n$. Using the natural inclusion, the notion of proximity graphs can be naturally extended as follows: given $\mathcal{G}$, we define (with a slight abuse of notation)

$$\mathcal{G} = \mathcal{G} \circ i_{\mathbb{F}} : X^n \to \mathbb{G}(X).$$

Additionally, we define the set of neighbors map $\mathcal{N}_{\mathcal{G}} : X \times X^n \to \mathbb{F}(X)$ by

$$\mathcal{N}_{\mathcal{G}}(p, (p_1, \ldots, p_n)) = \mathcal{N}_{\mathcal{G}}(p, i_{\mathbb{F}}(p_1, \ldots, p_n)).$$

According to this definition, coincident points in the tuple $(p_1, \ldots, p_n)$ will have the same set of neighbors. As before, it is convenient to define the shorthand notation $\mathcal{N}_{\mathcal{G},p} : X^n \to \mathbb{F}(X)$, $\mathcal{N}_{\mathcal{G},p}(P) = \mathcal{N}_{\mathcal{G}}(p, P)$ for $p \in X$.

2.2.4 Spatially distributed maps

Given a set Y and a proximity graph $\mathcal{G}$, a map $T : X^n \to Y^n$ is *spatially distributed over* $\mathcal{G}$ if there exists a map $\tilde{T} : X \times \mathbb{F}(X) \to Y$, with the property that, for all $(p_1, \ldots, p_n) \in X^n$ and for all $j \in \{1, \ldots, n\}$,

$$T_j(p_1, \ldots, p_n) = \tilde{T}(p_j, \mathcal{N}_{\mathcal{G},p_j}(p_1, \ldots, p_n)),$$

where T_j denotes the jth component of T. In other words, the jth component of a spatially distributed map at $(p_1, \ldots, p_n)$ can be computed with only knowledge of the vertex p_j and the neighboring vertices in the undirected graph $\mathcal{G}(P)$.

When studying coordination tasks and coordination algorithms, it will be relevant to characterize the spatially distributed features of functions, vector fields, and set-valued maps with respect to suitable proximity graphs.

Remark 2.12 (Relationship with the notion of spatially distributed graphs). Note that the proximity graph $\mathcal{G}_1$ is spatially distributed over the proximity graph $\mathcal{G}_2$ if and only if the map

$$P \in X^n \mapsto (\mathcal{N}_{\mathcal{G}_1,p_1}(P), \ldots, \mathcal{N}_{\mathcal{G}_1,p_n}(P)) \in \mathbb{F}(X)^n$$

is spatially distributed over $\mathcal{G}_2$. •

2.3 GEOMETRIC OPTIMIZATION PROBLEMS AND MULTICENTER FUNCTIONS

In this section we consider various interesting geometric optimization problems. By geometric optimization, we mean an optimization problem induced

by a collection of geometric objects (see Boltyanski et al., 1999). We shall pay particular attention to facility location problems, in which service sites are spatially allocated to fulfill a particular request.

2.3.1 Expected-value multicenter functions

Let $S \subset \mathbb{R}^d$ be a bounded environment of interest, and consider a density function $\phi : \mathbb{R}^d \to \mathbb{R}_{\geq 0}$. For the discussion of this section, only the value of ϕ restricted to S is of interest. One can regard ϕ as a function measuring the probability that some event takes place over the environment. The larger the value of $\phi(q)$, the more important the location q is. We refer to a non-increasing and piecewise continuously differentiable function $f : \mathbb{R}_{\geq 0} \to \mathbb{R}$, possibly with finite jump discontinuities, as a *performance*. Performance functions describe the utility of placing a node at a certain distance from a location in the environment. The smaller the distance, the larger the value of f, that is, the better the performance. For instance, in servicing problems, performance functions can encode the travel time or the energy expenditure required to service a specific destination. In sensing problems, performance functions can encode the signal-to-noise ratio between a source with an unknown location and a sensor attempting to locate it.

Given a bounded measurable set $S \subset \mathbb{R}^d$, a density function ϕ, and a performance function f, let us consider the expected value of the coverage over any point in S provided by a set of points $p_1, \ldots, p_n$. Formally, we define the *expected-value multicenter* function $\mathcal{H}_{\text{exp}} : S^n \to \mathbb{R}$ by

$$\mathcal{H}_{\text{exp}}(p_1, \ldots, p_n) = \int_S \max_{i \in \{1,\ldots,n\}} f(\|q - p_i\|_2)\phi(q)dq. \tag{2.3.1}$$

The definition of $\mathcal{H}_{\text{exp}}$ can be interpreted as follows: for each location $q \in S$, consider the best coverage of q among those provided by each of the nodes $p_1, \ldots, p_n$, which corresponds to the value $\max_{i \in \{1,\ldots,n\}} f(\|q - p_i\|_2)$. Then, evaluate the performance by the importance $\phi(q)$ of the location q. Finally, sum the resulting quantity over all the locations of the environment S, to obtain $\mathcal{H}_{\text{exp}}(p_1, \ldots, p_n)$ as a measure of the overall coverage provided by $p_1, \ldots, p_n$.

Given the meaning of $\mathcal{H}_{\text{exp}}$, we seek to solve the following geometric optimization problem:

$$\text{maximize } \mathcal{H}_{\text{exp}}(p_1, \ldots, p_n), \tag{2.3.2}$$

that is, we seek to determine a set of configurations $p_1, \ldots, p_n$ that maximize the value of the multicenter function $\mathcal{H}_{\text{exp}}$. An equivalent formulation of this problem is referred to as a *continuous p-median problem* in the literature

on facility location (see, e.g., Drezner, 1995). In our discussion, we will pay special attention to the case when $n = 1$, which we term the 1-*center* problem. For the purpose of solving (2.3.2), note that we can assume that the performance function satisfies $f(0) = 0$. This can be done without loss of generality, since for any $c \in \mathbb{R}$, one has

$$\int_S \max_{i\in\{1,\dots,n\}} (f(\|q - p_i\|_2) + c)\phi(q)dq = \mathcal{H}_{\text{exp}}(p_1, \dots, p_n) + c\, \mathrm{A}_\phi(S).$$

The expected-value multicenter function can be alternatively described in terms of the Voronoi partition of S generated by $\mathcal{P} = \{p_1, \dots, p_n\}$. Let us define the set

$$\mathcal{S}_{\text{coinc}} = \{(p_1, \dots, p_n) \in (\mathbb{R}^d)^n \mid p_i = p_j \text{ for some } i \neq j\},$$

consisting of tuples of n points, where some of them are repeated. Then, for $(p_1, \dots, p_n) \in S^n \setminus \mathcal{S}_{\text{coinc}}$, one has

$$\mathcal{H}_{\text{exp}}(p_1, \dots, p_n) = \sum_{i=1}^{n} \int_{V_i(\mathcal{P})} f(\|q - p_i\|_2)\phi(q)dq. \tag{2.3.3}$$

This expression of $\mathcal{H}_{\text{exp}}$ is appealing because it clearly shows the result of the overall coverage of the environment as the aggregate contribution of all individual nodes. If $(p_1, \dots, p_n) \in \mathcal{S}_{\text{coinc}}$, then a similar decomposition of $\mathcal{H}_{\text{exp}}$ can be written in terms of the distinct points $\mathcal{P} = i_{\mathbb{F}}(p_1, \dots, p_n)$.

Inspired by the expression (2.3.3), let us define a more general version of the expected-value multicenter function. Given $(p_1, \dots, p_n) \in S^n$ and a partition $\{W_1, \dots, W_n\} \subset \mathbb{P}(S)$ of S, let

$$\mathcal{H}_{\text{exp}}(p_1, \dots, p_n, W_1, \dots, W_n) = \sum_{i=1}^{n} \int_{W_i} f(\|q - p_i\|_2)\phi(q)dq. \tag{2.3.4}$$

Notice that $\mathcal{H}_{\text{exp}}(p_1, \dots, p_n) = \mathcal{H}_{\text{exp}}(p_1, \dots, p_n, V_1(\mathcal{P}), \dots, V_n(\mathcal{P}))$, for all $(p_1, \dots, p_n) \in S^n \setminus \mathcal{S}_{\text{coinc}}$. Moreover, one can establish the following optimality result (see Du et al., 1999).

Proposition 2.13 ($\mathcal{H}_{\text{exp}}$-optimality of the Voronoi partition). *Let $\mathcal{P} = \{p_1, \dots, p_n\} \in \mathbb{F}(S)$. For any performance function f and for any partition $\{W_1, \dots, W_n\} \subset \mathbb{P}(S)$ of S,*

$$\mathcal{H}_{\text{exp}}(p_1, \dots, p_n, V_1(\mathcal{P}), \dots, V_n(\mathcal{P})) \geq \mathcal{H}_{\text{exp}}(p_1, \dots, p_n, W_1, \dots, W_n),$$

and the inequality is strict if any set in $\{W_1, \dots, W_n\}$ differs from the corresponding set in $\{V_1(\mathcal{P}), \dots, V_n(\mathcal{P})\}$ by a set of positive measure. In other words, the Voronoi partition $\mathcal{V}(\mathcal{P})$ is optimal for $\mathcal{H}_{\text{exp}}$ among all partitions of S.

Proof. Assume that, for $i \neq j \in \{1, \dots, n\}$, the set $\text{int}(W_i) \cap \text{int}(V_j(\mathcal{P}))$ has strictly positive measure. For all $q \in \text{int}(W_i) \cap \text{int}(V_j(\mathcal{P}))$, we know that $\|q-p_i\|_2 > \|q-p_j\|_2$. Because f is non-increasing, $f(\|q-p_i\|_2) < f(\|q-p_j\|_2)$ and, since $\text{int}(W_i) \cap \text{int}(V_j(\mathcal{P}))$ has strictly positive measure,

$$\int_{\text{int}(W_i) \cap \text{int}(V_j(\mathcal{P}))} f(\|q-p_i\|_2)\phi(q)dq < \int_{\text{int}(W_i) \cap \text{int}(V_j(\mathcal{P}))} f(\|q-p_j\|_2)\phi(q)dq.$$

Therefore, we deduce

$$\int_{W_i} f(\|q-p_i\|_2)\phi(q)dq < \sum_{j=1}^{n} \int_{W_i \cap V_j(\mathcal{P})} f(\|q-p_j\|_2)\phi(q)dq,$$

and the statements follow. ■

Different performance functions lead to different expected-value multicenter functions. Let us examine some important cases.

Distortion problem: Consider the performance function $f(x) = -x^2$. Then, on $S^n \setminus \mathcal{S}_{\text{coinc}}$, the expected-value multicenter function takes the form

$$\mathcal{H}_{\text{dist}}(p_1, \dots, p_n) = -\sum_{i=1}^{n} \int_{V_i(P)} \|q-p_i\|_2^2 \phi(q)dq = -\sum_{i=1}^{n} \text{J}_\phi(V_i(\mathcal{P}), p_i),$$

where recall that $\text{J}_\phi(W, p)$ denotes the polar moment of inertia of the set W about the point p. In signal compression $-\mathcal{H}_{\text{dist}}$ is referred to as the *distortion function* and is relevant in many disciplines including vector quantization, signal compression, and numerical integration (see Gray and Neuhoff, 1998; Du et al., 1999). Here, distortion refers to the average deformation (weighted by the density ϕ) caused by reproducing $q \in S$ with the location p_i in $\mathcal{P} = \{p_1, \dots, p_n\}$ such that $q \in V_i(\mathcal{P})$. It is interesting to note that

$$\begin{aligned}\mathcal{H}_{\text{dist}}(p_1, \dots, p_n, W_1, \dots, W_n) &= -\sum_{i=1}^{n} \text{J}_\phi(W_i, p_i) \\ &= -\sum_{i=1}^{n} \text{J}_\phi(W_i, \text{CM}_\phi(W_i)) - \sum_{i=1}^{n} \text{A}_\phi(W_i)\|p_i - \text{CM}_\phi(W_i)\|_2^2, \quad (2.3.5)\end{aligned}$$

where in the last equality we have used the Parallel Axis Theorem (Hibbeler, 2006). Note that the first term only depends on the partition of S, whereas the second term also depends on the location of the points. The following result is a consequence of this observation.

Proposition 2.14 ($\mathcal{H}_{\text{dist}}$-optimality of centroid locations). *Let $\{W_1, \dots, W_n\} \subset \mathbb{P}(S)$ be a partition of S. Then, for any set points $\mathcal{P} = \{p_1, \dots, p_n\} \in \mathbb{F}(S)$,*

$$\mathcal{H}_{\text{dist}}\big(\operatorname{CM}_\phi(W_1), \dots, \operatorname{CM}_\phi(W_n), W_1, \dots, W_n\big) \geq \mathcal{H}_{\text{dist}}(p_1, \dots, p_n, W_1, \dots, W_n),$$

and the inequality is strict if there exists $i \in \{1, \dots, n\}$ for which W_i has non-vanishing area and $p_i \neq \operatorname{CM}_\phi(W_i)$. In other words, the centroid locations $\operatorname{CM}_\phi(W_1), \dots, \operatorname{CM}_\phi(W_n)$ are optimal for $\mathcal{H}_{\text{dist}}$ among all configurations in S.

A consequence of this result is that for the 1-center problem, that is, when $n = 1$, the node location that optimizes $p \mapsto \mathcal{H}_{\text{dist}}(p) = -\operatorname{J}_\phi(S, p)$ is the centroid of the set S, denoted by $\operatorname{CM}_\phi(S)$.

Area problem: For $a \in \mathbb{R}_{>0}$, consider the performance function $f(x) = 1_{[0,a]}(x)$, that is, the indicator function of the closed interval $[0, a]$. Then, the expected-value multicenter function takes the form

$$\begin{aligned}\mathcal{H}_{\text{area},a}(p_1, \dots, p_n) &= \sum_{i=1}^n \int_{V_i(\mathcal{P})} 1_{[0,a]}(\|q - p_i\|_2)\phi(q)dq \\ &= \sum_{i=1}^n \int_{V_i(\mathcal{P}) \cap \overline{B}(p_i,a)} \phi(q)dq \\ &= \sum_{i=1}^n \operatorname{A}_\phi(V_i(\mathcal{P}) \cap \overline{B}(p_i, a)) = \operatorname{A}_\phi(\cup_{i=1}^n \overline{B}(p_i, a)),\end{aligned}$$

that is, it corresponds to the area, measured according to ϕ, covered by the union of the n balls $\overline{B}(p_1, a), \dots, \overline{B}(p_n, a)$. Exercise E2.5 discusses the 1-center area problem.

Mixed distortion-area problem: For $a \in \mathbb{R}_{>0}$ and $b \leq -a^2$, consider the performance function $f(x) = -x^2\, 1_{[0,a]}(x) + b \cdot 1_{]a,+\infty[}(x)$. Then, on $S^n \setminus \mathcal{S}_{\text{coinc}}$, the expected-value multicenter function takes the form

$$\mathcal{H}_{\text{dist-area},a,b}(p_1, \dots, p_n) = -\sum_{i=1}^n \operatorname{J}_\phi(V_{i,a}(\mathcal{P}), p_i) + b \operatorname{A}_\phi(Q \setminus \cup_{i=1}^n \overline{B}(p_i, a)),$$

that is, it is a combination of the multicenter functions corresponding to the distortion problem and the area problem. Of special interest to us is the multicenter function that results from the choice $b = -a^2$. In this case, the performance function f is continuous, and we simply write $\mathcal{H}_{\text{dist-area},a}$. The extension of this function to sets of points and

partitions of the space reads as follows:

$$\mathcal{H}_{\text{dist-area},a}(p_1,\dots,p_n,W_1,\dots,W_n) = -\sum_{i=1}^{n}\Big(\mathrm{J}_\phi(W_i\cap\overline{B}(p_i,a),p_i)+a^2\,\mathrm{A}_\phi(W_i\cap(S\setminus\overline{B}(p_i,a)))\Big).$$

We leave the proof of the following optimality result as a guided exercise for the reader (see Exercise E2.10).

Proposition 2.15 ($\mathcal{H}_{\text{dist-area},a}$-optimality of centroid locations). *Let $\{W_1,\dots,W_n\}\subset\mathbb{P}(S)$ be a partition of S. Then, for any $\mathcal{P}=\{p_1,\dots,p_n\}\in\mathbb{F}(S)$,*

$$\mathcal{H}_{\text{dist-area},a}(q_1^*,\dots,q_n^*,W_1,\dots,W_n) \geq \mathcal{H}_{\text{dist-area},a}(p_1,\dots,p_n,W_1,\dots,W_n),$$

where we have used the shorthands $q_i^*=\mathrm{CM}_\phi(W_i\cap\overline{B}(p_i,a))$, for $i\in\{1,\dots,n\}$. Furthermore, the inequality is strict if there exists $i\in\{1,\dots,n\}$ for which W_i has non-vanishing area and $p_i\neq q_i^*$.

A consequence of this result is that for the 1-center problem, that is, when $n=1$—the node location that optimizes $p\mapsto\mathcal{H}_{\text{dist-area},a}(p)=\mathrm{J}_\phi(S\cap\overline{B}(p,a),p)+a^2\,\mathrm{A}_\phi(S\setminus\overline{B}(p,a))$ is the centroid of the set $S\cap\overline{B}(p,a)$, denoted by $\mathrm{CM}_\phi(S\cap\overline{B}(p,a))$.

Next, we characterize the smoothness of the expected-value multicenter function. Before stating the precise result, let us introduce some useful notation. For a performance function f, let $\mathrm{Dscn}(f)$ denote the (finite) set of points where f is discontinuous. For each $a\in\mathrm{Dscn}(f)$, define the limiting values from the left and from the right, respectively, as

$$f_-(a)=\lim_{x\to a^-}f(x),\qquad f_+(a)=\lim_{x\to a^+}f(x).$$

We are now ready to characterize the smoothness of $\mathcal{H}_{\text{exp}}$, whose proof is given in Section 2.5.3. Before stating the result, recall that the line integral of a function $g:\mathbb{R}^2\to\mathbb{R}$ over a curve C parameterized by a continuous and piecewise continuously differentiable map $\gamma:[0,1]\to\mathbb{R}^2$ is defined by

$$\int_C g=\int_C g(\gamma)d\gamma:=\int_0^1 g(\gamma(t))\,\|\dot\gamma(t)\|_2\,dt,$$

and is independent of the selected parameterization.

Theorem 2.16 (Smoothness properties of $\mathcal{H}_{\text{exp}}$). *Given a set $S\subset\mathbb{R}^d$ that is bounded and measurable, a density $\phi:\mathbb{R}\to\mathbb{R}_{\geq0}$, and a performance function $f:\mathbb{R}_{\geq0}\to\mathbb{R}$, the expected-value multicenter function $\mathcal{H}_{\text{exp}}:S^n\to\mathbb{R}$ is*

(i) globally Lipschitz[2] *on* S^n*; and*

(ii) continuously differentiable on $S^n \setminus \mathcal{S}_{\text{coinc}}$*, where for* $i \in \{1, \dots, n\}$

$$\frac{\partial \mathcal{H}_{\text{exp}}}{\partial p_i}(P) = \int_{V_i(\mathcal{P})} \frac{\partial}{\partial p_i} f(\|q - p_i\|_2)\phi(q)dq + \sum_{a \in \text{Dscn}(f)} \big(f_-(a) - f_+(a)\big) \int_{V_i(\mathcal{P}) \cap \partial \overline{B}(p_i,a)} \text{n}_{\text{out}}(q)\phi(q)dq, \quad (2.3.6)$$

where n_{out} *is the outward normal vector to* $\overline{B}(p_i, a)$*. Therefore, the gradient of* $\mathcal{H}_{\text{exp}}$*, interpreted as a map from* S^n *to* $\mathbb{R}^n$*, is spatially distributed (in the sense defined in Section 2.2.4) over the Delaunay graph* $\mathcal{G}_{\text{D}}$*.*

Let us discuss how Theorem 2.16 particularizes to the distortion, area, and mixed distortion-area problems.

Distortion problem: In this case, the performance function does not have any discontinuities and, therefore, the second term in (2.3.6) vanishes. The gradient of $\mathcal{H}_{\text{dist}}$ on $S^n \setminus \mathcal{S}_{\text{coinc}}$ then takes the form, for each $i \in \{1, \dots, n\}$,

$$\frac{\partial \mathcal{H}_{\text{dist}}}{\partial p_i}(P) = 2\,\text{A}_\phi(V_i(\mathcal{P}))(\text{CM}_\phi(V_i(\mathcal{P})) - p_i),$$

that is, the ith component of the gradient points in the direction of the vector going from p_i to the centroid of its Voronoi cell. The critical points of $\mathcal{H}_{\text{dist}}$ are therefore the set of centroidal Voronoi configurations in S (cf. Section 2.1.4). This is a natural generalization of the result for the 1-center case, where the optimal node location is the centroid $\text{CM}_\phi(S)$.

Area problem: In this case, the performance function is differentiable everywhere except at a single discontinuity, and its derivative is identically zero. Therefore, the first term in (2.3.6) vanishes. The gradient of $\mathcal{H}_{\text{area},a}$ on $S^n \setminus \mathcal{S}_{\text{coinc}}$ then takes the form, for each $i \in \{1, \dots, n\}$,

$$\frac{\partial \mathcal{H}_{\text{area},a}}{\partial p_i}(P) = \int_{V_i(\mathcal{P}) \cap \partial \overline{B}(p_i,a)} \text{n}_{\text{out}}(q)\phi(q)dq,$$

where n_{out} is the outward normal vector to $\overline{B}(p_i, a)$. The gradient is an average of the normal at each point of $V_i(\mathcal{P}) \cap \partial\overline{B}(p_i, a)$, as illustrated in Figure 2.13. The critical points of $\mathcal{H}_{\text{area},a}$ correspond to configurations with the property that each p_i is a local maximum for the area of $V_{i,a}(P) = V_i(P) \cap \overline{B}(p_i, a)$ at fixed $V_i(P)$. We refer to these

[2] Given $S \subset \mathbb{R}^h$, a function $f : S \to \mathbb{R}^k$ is globally Lipschitz if there exists $K \in \mathbb{R}_{>0}$ such that $\|f(x - y)\|_2 \leq K\|x - y\|_2$ for all $x, y \in S$.

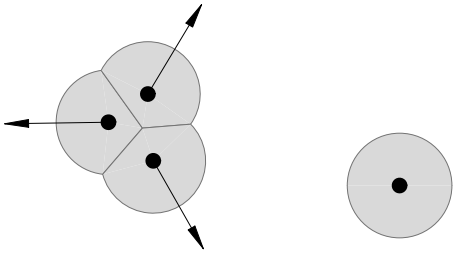

Figure 2.13 The gradient of the area function when the density function is constant. The component of the gradient corresponding to the rightmost node is zero; there is no incentive for this node to move in any particular direction. The component of the gradient for each of the three leftmost agents is non-zero; roughly speaking, by moving along the gradient directions, these agents decrease the overlapping among their respective disk and cover new regions of the space.

configurations as *a-limited area-centered* Voronoi configurations. This is a natural generalization of the result for the 1-center case, where the optimal node location maximizes $\mathrm{A}_\phi(S \cap \overline{B}(p,a))$ (cf., Exercise E2.5).

Mixed distortion-area problem: In this case, the gradient of the multicenter function $\mathcal{H}_{\text{dist-area},a,b}$ is a combination of the gradients of $\mathcal{H}_{\text{dist}}$ and $\mathcal{H}_{\text{area},a}$. Specifically, one has for each $i \in \{1,\dots,n\}$,

$$\frac{\partial \mathcal{H}_{\text{dist-area},a,b}}{\partial p_i}(P) = 2\,\mathrm{A}_\phi(V_{i,a}(\mathcal{P}))(\mathrm{CM}_\phi(V_{i,a}(\mathcal{P})) - p_i) \\ - (a^2+b)\int_{V_i(\mathcal{P})\cap \partial\overline{B}(p_i,a)} \mathrm{n}_{\text{out}}(q)\phi(q)dq,$$

where n_{out} is the outward normal vector to $\overline{B}(p_i,a)$. For the particular case when $b=-a^2$, the performance function is continuous, and the gradient of $\mathcal{H}_{\text{dist-area},a}$ takes the simpler form

$$\frac{\partial \mathcal{H}_{\text{dist-area},a}}{\partial p_i}(P) = 2\,\mathrm{A}_\phi(V_{i,a}(\mathcal{P}))(\mathrm{CM}_\phi(V_{i,a}(\mathcal{P})) - p_i),$$

which points in the direction of the vector from p_i to the centroid of its a-limited Voronoi cell. In this case, the critical points of $\mathcal{H}_{\text{dist-area},a}$ are therefore the set of a-limited centroidal Voronoi configurations in S (cf., Section 2.1.4). This is a natural generalization of the result for the 1-center case, where the optimal node location is the centroid $\mathrm{CM}_\phi(S \cap \overline{B}(p,a))$.

We refer to $\mathcal{H}_{\text{dist}}$, $\mathcal{H}_{\text{area},a}$, and $\mathcal{H}_{\text{dist-area},a}$ as multicenter functions because, as the above discussion shows, their critical points correspond to various notions of center Voronoi configurations.

Note that the gradients of $\mathcal{H}_{\text{area},a}$ and $\mathcal{H}_{\text{dist-area},a,b}$ are spatially distributed over the $2a$-limited Delaunay graph $\mathcal{G}_{\text{LD}}(2a)$. This observation is important for practical considerations: robotic agents with range-limited interactions cannot in general compute the gradient of $\mathcal{H}_{\text{dist}}$ because, as we noted in Remark 2.10, for a given $r \in \mathbb{R}_{>0}$, $\mathcal{G}_{\text{D}}$ is not in general spatially distributed over $\mathcal{G}_{\text{disk}}(r)$. However, robotic agents with range-limited interactions can compute the gradients of $\mathcal{H}_{\text{area},a}$ and $\mathcal{H}_{\text{dist-area},a,b}$ as long as $r \geq 2a$ because, from Theorem 2.7(iii), $\mathcal{G}_{\text{LD}}(r)$ is spatially distributed over $\mathcal{G}_{\text{disk}}(r)$. The relevance of this fact is further justified by the following result.

Proposition 2.17 (Constant-factor approximation of $\mathcal{H}_{\text{dist}}$). *Let $S \subset \mathbb{R}^d$ be bounded and measurable. Consider the mixed distortion-area problem with $a \in]0, \operatorname{diam} S]$ and $b = -\operatorname{diam}(S)^2$. Then, for all $P \in S^n$,*

$$\mathcal{H}_{\text{dist-area},a,b}(P) \leq \mathcal{H}_{\text{dist}}(P) \leq \beta^2 \, \mathcal{H}_{\text{dist-area},a,b}(P) < 0, \tag{2.3.7}$$

where $\beta = \frac{a}{\operatorname{diam}(S)} \in [0, 1]$.

In fact, similar constant-factor approximations of the expected-value multicenter function $\mathcal{H}_{\text{exp}}$ can also be established (see Cortés et al., 2005).

2.3.2 Worst-case and disk-covering multicenter functions

Given a compact set $S \subset \mathbb{R}^d$ and a performance function f, let us consider the point in S that is worst covered by a set of points $p_1, \ldots, p_n$. Formally, we define the *worst-case multicenter* function $\mathcal{H}_{\text{worst}} : S^n \to \mathbb{R}$ by

$$\mathcal{H}_{\text{worst}}(p_1, \ldots, p_n) = \min_{q \in S} \max_{i \in \{1,\ldots,n\}} f(\|q - p_i\|_2). \tag{2.3.8}$$

The definition of $\mathcal{H}_{\text{worst}}$ can be read as follows: for each location $q \in S$, consider the best coverage of q among those provided by each of the nodes $p_1, \ldots, p_n$, which corresponds to the value $\max_{i \in \{1,\ldots,n\}} f(\|q - p_i\|_2)$. Then, compute the worst coverage $\mathcal{H}_{\text{worst}}(p_1, \ldots, p_n)$ by comparing the performance at all locations in S.

Given the interpretation of $\mathcal{H}_{\text{worst}}$, we seek to solve the following geometric optimization problem:

$$\text{maximize } \mathcal{H}_{\text{worst}}(p_1, \ldots, p_n), \tag{2.3.9}$$

that is, we seek to determine configurations $p_1, \ldots, p_n$ that maximize the value of $\mathcal{H}_{\text{worst}}$. An equivalent formulation of this problem is referred to as a *continuous p-center problem* in the literature on facility location (see, e.g., Drezner, 1995).

In the present context, also relevant is the *disk-covering multicenter* function $\mathcal{H}_{\text{dc}} : S^n \to \mathbb{R}$, defined by

$$\mathcal{H}_{\text{dc}}(p_1, \ldots, p_n) = \max_{q \in S} \min_{i \in \{1,\ldots,n\}} \|q - p_i\|_2. \tag{2.3.10}$$

The value of $\mathcal{H}_{\text{dc}}$ can be interpreted as the largest possible distance from a point in S to one of the locations $p_1, \ldots, p_n$. Note that, by definition, the environment S is contained in the union of n closed balls centered at $p_1, \ldots, p_n$ with radius $\mathcal{H}_{\text{dc}}(p_1, \ldots, p_n)$. The definition of $\mathcal{H}_{\text{dc}}$ is illustrated in Figure 2.14(a).

The following result establishes the relationship between the worst-case and the disk-covering multicenter functions, and as byproduct, provides an elegant reformulation of the geometric optimization problem (2.3.9). Its proof is left to the reader.

Lemma 2.18 (Relationship between $\mathcal{H}_{\text{worst}}$ and $\mathcal{H}_{\text{dc}}$). *Given $S \subset \mathbb{R}^d$ compact and a performance function $f : \mathbb{R}_{\geq 0} \to \mathbb{R}$, one has $\mathcal{H}_{\text{worst}} = f \circ \mathcal{H}_{\text{dc}}$.*

Using Lemma 2.18 and the fact that f is non-increasing, we can reformulate the geometric optimization problem (2.3.9) as

$$\text{minimize } \mathcal{H}_{\text{dc}}(p_1, \ldots, p_n), \tag{2.3.11}$$

that is, find the minimum radius r such that the environment S is covered by n closed balls centered at $p_1, \ldots, p_n$ with equal radius r. Note the connection between this formulation and the classical disk-covering problem: how to cover a region with (possibly overlapping) disks of minimum radius. We shall comment more on this connection later.

Because of the equivalence between the geometric optimization problems (2.3.9) and (2.3.11), we focus our attention on $\mathcal{H}_{\text{dc}}$. The disk-covering multicenter function can be alternatively described in terms of the Voronoi partition of S generated by $\mathcal{P} = \{p_1, \ldots, p_n\}$. For $(p_1, \ldots, p_n) \in S^n \setminus \mathcal{S}_{\text{coinc}}$,

$$\begin{aligned} \mathcal{H}_{\text{dc}}(p_1, \ldots, p_n) &= \max_{i \in \{1,\ldots,n\}} \max_{q \in V_i(\mathcal{P})} \|q - p_i\|_2 \\ &= \max_{i \in \{1,\ldots,n\}} \max_{q \in \partial V_i(\mathcal{P})} \|q - p_i\|_2. \end{aligned} \tag{2.3.12}$$

This characterization of $\mathcal{H}_{\text{dc}}$ is illustrated in Figure 2.14(b). The expression (2.3.12) is appealing because it clearly shows the value of $\mathcal{H}_{\text{dc}}$ as the result of the aggregate contribution of all individual nodes. If $(p_1, \ldots, p_n) \in \mathcal{S}_{\text{coinc}}$, then a similar decomposition of $\mathcal{H}_{\text{dc}}$ can be written in terms of the distinct points $\mathcal{P} = i_{\mathbb{F}}(p_1, \ldots, p_n)$. A node $i \in \{1, \ldots, n\}$ is called *active* at $(p_1, \ldots, p_n)$ if $\max_{q \in \partial V_i(\mathcal{P})} \|q - p_i\|_2 = \mathcal{H}_{\text{dc}}(p_1, \ldots, p_n)$. A node is *passive* at $(p_1, \ldots, p_n)$ if it is not active.

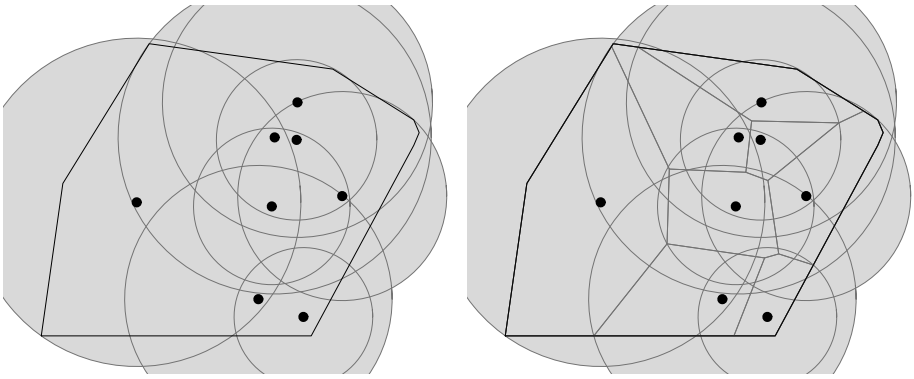

(a) (b)

Figure 2.14 An illustration of the definition of $\mathcal{H}_{\mathrm{dc}}$: (a) and (b) show the same configuration, with and without the Voronoi configuration, respectively. For each node, the disk is the minimum-radius disk centered at the node and enclosing the Voronoi cell. The value of $\mathcal{H}_{\mathrm{dc}}$ is the radius of the disk centered at the leftmost node.

Inspired by expression (2.3.12), let us define a more general version of the disk-covering multicenter function. Given $(p_1, \ldots, p_n) \in S^n$ and a partition $\{W_1, \ldots, W_n\} \subset \mathbb{P}(S)$ of S, let

$$\mathcal{H}_{\mathrm{dc}}(p_1, \ldots, p_n, W_1, \ldots, W_n) = \max_{i \in \{1,\ldots,n\}} \max_{q \in \partial W_i} \|q - p_i\|_2.$$

Note the relationship $\mathcal{H}_{\mathrm{dc}}(p_1, \ldots, p_n) = \mathcal{H}_{\mathrm{dc}}(p_1, \ldots, p_n, V_1(\mathcal{P}), \ldots, V_n(\mathcal{P}))$, for all $(p_1, \ldots, p_n) \in S^n \setminus \mathcal{S}_{\mathrm{coinc}}$. Moreover, one can establish the following optimality result, whose proof is given in Section 2.5.4.

Proposition 2.19 ($\mathcal{H}_{\mathrm{dc}}$-optimality of the Voronoi partition and circumcenter locations). *For any $\mathcal{P} = \{p_1, \ldots, p_n\} \in \mathbb{F}(S)$ and any partition $\{W_1, \ldots, W_n\} \subset \mathbb{P}(S)$ of S,*

$$\mathcal{H}_{\mathrm{dc}}(p_1, \ldots, p_n, V_1(\mathcal{P}), \ldots, V_n(\mathcal{P})) \leq \mathcal{H}_{\mathrm{dc}}(p_1, \ldots, p_n, W_1, \ldots, W_n),$$

that is, the Voronoi partition $\mathcal{V}(\mathcal{P})$ is optimal for $\mathcal{H}_{\mathrm{dc}}$ among all partitions of S, and

$$\mathcal{H}_{\mathrm{dc}}(\mathrm{CC}(W_1), \ldots, \mathrm{CC}(W_n), W_1, \ldots, W_n) \leq \mathcal{H}_{\mathrm{dc}}(p_1, \ldots, p_n, W_1, \ldots, W_n),$$

that is, the circumcenter locations $\mathrm{CC}(W_1), \ldots, \mathrm{CC}(W_n)$ are optimal for $\mathcal{H}_{\mathrm{dc}}$ among all configurations in S.

As a corollary of this result, we have that the circumcenter of S is a global optimum of $\mathcal{H}_{\mathrm{dc}}$ for the 1-center problem, that is, when $n = 1$. This comes as no surprise since, in this case, the value $\mathcal{H}_{\mathrm{dc}}(p)$ corresponds to the radius of the minimum-radius sphere centered at p that encloses S.

The following result characterizes the smoothness properties of the disk-covering multicenter function; for more details and for the proof, see Cortés and Bullo (2005).

Theorem 2.20 (Smoothness properties of $\mathcal{H}_{\mathrm{dc}}$). *Given $S \subset \mathbb{R}^d$ compact, the disk-covering multicenter function $\mathcal{H}_{\mathrm{dc}} : S^n \to \mathbb{R}$ is globally Lipschitz on S^n.*

The generalized gradient and the critical points of $\mathcal{H}_{\mathrm{dc}}$ can be characterized, but require a careful study based on nonsmooth analysis (Clarke, 1983). In particular, two facts taken from Cortés and Bullo (2005) are of interest here. First, under certain technical conditions, one can show that the critical points of $\mathcal{H}_{\mathrm{dc}}$ are circumcenter Voronoi configurations. This is why we refer to $\mathcal{H}_{\mathrm{dc}}$ as a multicenter function. Second, the generalized gradient of $\mathcal{H}_{\mathrm{dc}}$ is not spatially distributed over $\mathcal{G}_{\mathrm{D}}$. This is essentially due to the inherent comparison among all agents that is embedded in the definition of $\mathcal{H}_{\mathrm{dc}}$ (via the max function).

2.3.3 Sphere-packing multicenter functions

Given a compact connected set $S \subset \mathbb{R}^d$, imagine trying to fit inside S "maximally large" non-intersecting balls. Assuming that the balls are centered at a set of points $p_1, \ldots, p_n$, we aim to maximize their smallest radius. We define the *sphere-packing multicenter* function $\mathcal{H}_{\mathrm{sp}} : S^n \to \mathbb{R}$ by

$$\mathcal{H}_{\mathrm{sp}}(p_1, \ldots, p_n) = \min_{i \neq j \in \{1,\ldots,n\}} \Big\{ \frac{1}{2}\|p_i - p_j\|_2, \operatorname{dist}(p_i, \partial S) \Big\}. \tag{2.3.13}$$

The definition of $\mathcal{H}_{\mathrm{sp}}$ can be read as follows: consider the pairwise distances between any two points p_i, p_j (multiplied by a factor $1/2$ so that each point can fit a ball of equal radius and these balls do not intersect), and the individual distances from each point to the boundary of the environment. The value of $\mathcal{H}_{\mathrm{sp}}$ is then the smallest of all distances, guaranteeing that the union of n open balls centered at $p_1, \ldots, p_n$ with radius $\mathcal{H}_{\mathrm{sp}}(p_1, \ldots, p_n)$ is disjoint and contained in S. The definition of $\mathcal{H}_{\mathrm{sp}}$ is illustrated in Figure 2.15(a).

Given the definition of $\mathcal{H}_{\mathrm{sp}}$, we seek to solve the following geometric optimization problem:

$$\text{maximize } \mathcal{H}_{\mathrm{sp}}(p_1, \ldots, p_n), \tag{2.3.14}$$

that is, we seek to determine configurations $p_1, \ldots, p_n$ that maximize the value of $\mathcal{H}_{\mathrm{sp}}$. Note the connection of this formulation with the classical sphere-packing problem: how to maximize the number of fixed-radius non-overlapping spheres inside a region.

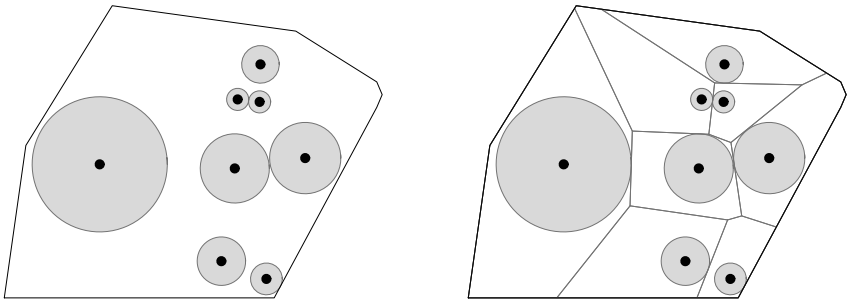

(a) (b)

Figure 2.15 An illustration of the definition of $\mathcal{H}_{\text{sp}}$: (a) and (b) show the same configuration, with and without the Voronoi configuration, respectively. For each node, the disk is the maximum-radius disk centered at the node and contained in the Voronoi cell. The value of $\mathcal{H}_{\text{sp}}$ is the radius of the two equal-radius smallest disks.

The sphere-packing multicenter function can be alternatively described in terms of the Voronoi partition of S generated by $\mathcal{P} = \{p_1, \ldots, p_n\}$. For $(p_1, \ldots, p_n) \in S^n \setminus \mathcal{S}_{\text{coinc}}$, one has

$$\mathcal{H}_{\text{sp}}(p_1, \ldots, p_n) = \min_{i \in \{1,\ldots,n\}} \min_{q \in \partial V_i(\mathcal{P})} \|q - p_i\|_2. \tag{2.3.15}$$

This description is illustrated in Figure 2.15(b). As for the previous multicenter functions, expression (2.3.15) is appealing because it clearly shows the value of of $\mathcal{H}_{\text{sp}}$ as the result of the aggregate contribution of all individual nodes. If $(p_1, \ldots, p_n) \in \mathcal{S}_{\text{coinc}}$, then a similar decomposition of $\mathcal{H}_{\text{sp}}$ exists in terms of the distinct points $\mathcal{P} = i_{\mathbb{F}}(p_1, \ldots, p_n)$. A node $i \in \{1, \ldots, n\}$ is called *active* at $(p_1, \ldots, p_n)$ if $\min_{q \in \partial V_i(\mathcal{P})} \|q - p_i\|_2 = \mathcal{H}_{\text{sp}}(p_1, \ldots, p_n)$. A node is *passive* at $(p_1, \ldots, p_n)$ if it is not active.

Inspired by expression (2.3.15), let us define a more general version of the sphere-packing multicenter function. Given $(p_1, \ldots, p_n) \in S^n$ and a partition $\{W_1, \ldots, W_n\} \subset \mathbb{P}(S)$ of S, let

$$\mathcal{H}_{\text{sp}}(p_1, \ldots, p_n, W_1, \ldots, W_n) = \min_{i \in \{1,\ldots,n\}} \min_{q \in \partial W_i} \|q - p_i\|_2.$$

Note the relationship $\mathcal{H}_{\text{sp}}(p_1, \ldots, p_n) = \mathcal{H}_{\text{sp}}(p_1, \ldots, p_n, V_1(\mathcal{P}), \ldots, V_n(\mathcal{P}))$, for all $(p_1, \ldots, p_n) \in S^n \setminus \mathcal{S}_{\text{coinc}}$. Additionally, note that the quantity $\mathcal{H}_{\text{sp}}(q_1, \ldots, q_n, W_1, \ldots, W_n)$ is the same for any $q_i \in \text{IC}(W_i)$, $i \in \{1, \ldots, n\}$. With a slight abuse of notation, we refer to this common value using the symbol $\mathcal{H}_{\text{sp}}(\text{IC}(W_1), \ldots, \text{IC}(W_n), W_1, \ldots, W_n)$. Moreover, one can establish the following optimality result (for the proof, see Section 2.5.5).

Proposition 2.21 ($\mathcal{H}_{\text{sp}}$-optimality of the Voronoi partition and incenter locations). *For any $\mathcal{P} = \{p_1, \ldots, p_n\} \in \mathbb{F}(S)$ and any partition $\{W_1, \ldots, W_n\} \subset \mathbb{P}(S)$ of S,*

$$\mathcal{H}_{\text{sp}}(p_1, \ldots, p_n, V_1(\mathcal{P}), \ldots, V_n(\mathcal{P})) \geq \mathcal{H}_{\text{sp}}(p_1, \ldots, p_n, W_1, \ldots, W_n),$$

that is, the Voronoi partition $\mathcal{V}(\mathcal{P})$ is optimal for $\mathcal{H}_{\text{sp}}$ among all partitions of S, and

$$\mathcal{H}_{\text{sp}}(\text{IC}(W_1), \ldots, \text{IC}(W_n), W_1, \ldots, W_n) \geq \mathcal{H}_{\text{sp}}(p_1, \ldots, p_n, W_1, \ldots, W_n),$$

that is, the incenters $\text{IC}(W_1), \ldots, \text{IC}(W_n)$ are optimal for $\mathcal{H}_{\text{sp}}$ among all configurations in S.

As a corollary of this result, we have that the incenter set of S is composed of global optima of $\mathcal{H}_{\text{sp}}$ for the 1-center problem, that is, when $n = 1$. This comes as no surprise since, in this case, the value $\mathcal{H}_{\text{sp}}(p)$ corresponds to the radius of the maximum-radius sphere centered at p enclosed in S. The following result characterizes the smoothness properties of the sphere-packing multicenter function (see Cortés and Bullo, 2005).

Theorem 2.22 (Smoothness properties of $\mathcal{H}_{\text{sp}}$). *Given $S \subset \mathbb{R}^d$ compact, the sphere-packing multicenter function $\mathcal{H}_{\text{sp}} : S^n \to \mathbb{R}$ is globally Lipschitz on S^n.*

We conclude this section with some remarks that are analogous to those for the function $\mathcal{H}_{\text{dc}}$. The generalized gradient and the critical points of $\mathcal{H}_{\text{sp}}$ can be characterized, but require a careful study based on nonsmooth analysis (Clarke, 1983). In particular, two facts taken from Cortés and Bullo (2005) are of interest here. First, under certain technical conditions, one can show that the critical points of $\mathcal{H}_{\text{sp}}$ are incenter Voronoi configurations. This is why we refer to $\mathcal{H}_{\text{sp}}$ as a multicenter function. Second, the generalized gradient of $\mathcal{H}_{\text{sp}}$ is not spatially distributed over $\mathcal{G}_{\text{D}}$. This is essentially due to the inherent comparison among all agents that is embedded in the definition of $\mathcal{H}_{\text{sp}}$ (via the min function).

2.4 NOTES

A thorough introduction to computational geometric concepts can be found in Preparata and Shamos (1993), de Berg et al. (2000), and O'Rourke (2000). The handbooks Goodman and O'Rourke (2004) and Sack and Urrutia (2000) present a comprehensive overview of computational geometric problems and their applications. Among the numerous topics that we do not discuss in this chapter, we mention distance geometry and rigidity theory (Whiteley, 1997), which are notable for their applications to network localization and formation control.

The notion of Voronoi partition, and generalizations of it, have been applied in numerous areas, including spatial interpolation, pattern analysis, spatial processes modeling, and optimization, to name a few. The survey Aurenhammer (1991) and the book by Okabe et al. (2000) discuss the history, properties, and applications of Voronoi partitions. The nearest-neighbor and natural-neighbor interpolations based on Voronoi partitions (see, for example Sibson, 1981; Boissonnat and Cazals, 2002) are of particular interest to the treatment of this chapter because of their spatially distributed computation character. Spatially distributed maps for motion coordination are discussed in Martínez et al. (2007) and adopted in later chapters.

Proximity graphs (Jaromczyk and Toussaint, 1992) are a powerful tool to capture the structure and shape of geometric objects, and therefore have applications in multiple areas, including topology control of wireless networks (Santi, 2005), computer graphics (Langetepe and Zachmann, 2006), and geographic analysis (Radke, 1988). The connectivity properties of certain proximity graphs (including those stated in Theorem 2.8) are taken from Cortés et al. (2005, 2006). In cooperative control, a closely related notion is that of state-dependent graph (Mesbahi, 2005). Random geometric graphs (Penrose, 2003) and percolation theory (Bollobás and Riordan, 2006; Meester and Roy, 2008) study the properties of proximity graphs associated to the random deployment of points according to some specified density function.

Locational optimization problems (Drezner, 1995; Drezner and Hamacher, 2001) are spatial resource-allocation problems (e.g., where to place mailboxes in a city, or where to place cache serves on the internet) that pervade a broad spectrum of scientific disciplines. Computational geometry plays an important role in locational optimization (Robert and Toussaint, 1990; Okabe et al., 2000). The field of geometric optimization (Mitchell, 1997; Agarwal and Sharir, 1998; Boltyanski et al., 1999) blends the geometric and locational optimization aspects to study a wide variety of optimization problems induced by geometric objects. The smoothness properties of the cost function $\mathcal{H}_{\text{exp}}$ are taken from Cortés et al. (2005).

2.5 PROOFS

This section gathers the proofs of the main results presented in the chapter.

2.5.1 Proofs of Theorem 2.7 and Theorem 2.8

Proof of Theorem 2.7. The inclusions in fact (i) are taken from Jaromczyk and Toussaint (1992), and de Berg et al. (2000). The proof of the first inclusion in fact (ii) is as follows. Let $(p_i, p_j) \in \mathcal{E}_{\mathcal{G}_{\mathrm{G}} \cap \mathcal{G}_{\mathrm{disk}}(r)}(\mathcal{P})$. From the definition of the Gabriel graph, we deduce that $\|\frac{p_i+p_j}{2} - p_i\|_2 = \|\frac{p_i+p_j}{2} - p_j\|_2 \leq \|\frac{p_i+p_j}{2} - p_k\|_2$, for all $k \in \{1, \dots, n\} \setminus \{i, j\}$, and therefore, $\frac{p_i+p_j}{2} \in V_i(\mathcal{P}) \cap V_j(\mathcal{P})$. Since $(p_i, p_j) \in \mathcal{E}_{\mathcal{G}_{\mathrm{disk}}(r)}(\mathcal{P})$, we deduce that $\frac{p_i+p_j}{2} \in \overline{B}(p_i, \frac{r}{2}) \cap \overline{B}(p_j, \frac{r}{2})$, and hence $(p_i, p_j) \in \mathcal{E}_{\mathcal{G}_{\mathrm{LD}}(r)}(\mathcal{P})$. The second inclusion in (ii) is straightforward: if $(p_i, p_j) \in \mathcal{E}_{\mathcal{G}_{\mathrm{LD}}(r)}(\mathcal{P})$, then $V_i(\mathcal{P}) \cap V_j(\mathcal{P}) \neq \emptyset$, that is, $(p_i, p_j) \in \mathcal{E}_{\mathcal{G}_{\mathrm{D}}}(\mathcal{P})$. Since clearly $(p_i, p_j) \in \mathcal{E}_{\mathcal{G}_{\mathrm{disk}}(r)}(\mathcal{P})$, we conclude (ii). ■

Proof of Theorem 2.8. The proof of fact (i) is as follows. Let $\mathcal{P} \in \mathbb{F}(\mathbb{R}^d)$. If $\mathcal{G}_{\mathrm{EMST}}(\mathcal{P}) \subseteq \mathcal{G}_{\mathrm{disk}}(r)(\mathcal{P})$, then clearly $\mathcal{G}_{\mathrm{disk}}(r)(\mathcal{P})$ is connected. To prove the other implication, we reason by contradiction. Assume $\mathcal{G}_{\mathrm{disk}}(r)(\mathcal{P})$ is connected and let $\mathcal{G}_{\mathrm{EMST}}(\mathcal{P}) \not\subseteq \mathcal{G}_{\mathrm{disk}}(r)(\mathcal{P})$, that is, there exist p_i and p_j with $(p_i, p_j) \in \mathcal{E}_{\mathcal{G}_{\mathrm{EMST}}}(\mathcal{P})$ and $\|p_i - p_j\|_2 > r$. If we remove this edge from $\mathcal{E}_{\mathcal{G}_{\mathrm{EMST}}}(\mathcal{P})$, then the tree becomes disconnected into two connected components T_1 and T_2, with $p_i \in T_1$ and $p_j \in T_2$. Now, since by hypothesis $\mathcal{G}_{\mathrm{disk}}(r)(\mathcal{P})$ is connected, there must exist $k, l \in \{1, \dots, n\}$ such that $p_k \in T_1$, $p_l \in T_2$ and $\|p_k - p_l\|_2 \leq r$. If we add the edge (p_k, p_l) to the set of edges of $T_1 \cup T_2$, then the resulting graph G is acyclic, connected, and contains all the vertices $\mathcal{P}$, that is, G is a spanning tree. Moreover, since $\|p_k - p_l\|_2 \leq r < \|p_i - p_j\|_2$ and T_1 and T_2 are induced subgraphs of $\mathcal{G}_{\mathrm{EMST}}(\mathcal{P})$, we conclude that G has smaller length than $\mathcal{G}_{\mathrm{EMST}}(\mathcal{P})$, which is a contradiction with the definition of the Euclidean minimum spanning tree.

Next, we prove fact (ii). For $r \in \mathbb{R}_+$, it suffices for us to show that $\mathcal{G}_{\mathrm{EMST}} \cap \mathcal{G}_{\mathrm{disk}}(r)$ has the same connected components as $\mathcal{G}_{\mathrm{disk}}(r)$, since this implies that the same result holds for $\mathcal{G}_{\mathrm{RN}} \cap \mathcal{G}_{\mathrm{disk}}(r)$, $\mathcal{G}_{\mathrm{G}} \cap \mathcal{G}_{\mathrm{disk}}(r)$, and $\mathcal{G}_{\mathrm{LD}}(r)$. Since $\mathcal{G}_{\mathrm{EMST}} \cap \mathcal{G}_{\mathrm{disk}}(r)$ is a subgraph of $\mathcal{G}_{\mathrm{disk}}(r)$, it is clear that vertices belonging to the same connected component of $\mathcal{G}_{\mathrm{EMST}} \cap \mathcal{G}_{\mathrm{disk}}(r)$ must also belong to the same connected component of $\mathcal{G}_{\mathrm{disk}}(r)$. To prove the converse, let $\mathcal{P} \in \mathbb{F}(\mathbb{R}^d)$, and assume that p_i and p_j in $\mathcal{P}$ verify $\|p_i - p_j\|_2 \leq r$. Let C be the connected component of $\mathcal{G}_{\mathrm{disk}}(r)(\mathcal{P})$ to which they belong. With a slight abuse of notation, we also denote by C the vertices of the connected component. Since C is connected, then $\mathcal{G}_{\mathrm{EMST}}(C) \subset C$ by fact (i). Moreover, since all the nodes in $\mathcal{P} \setminus C$ are at a distance strictly larger than r from any node of C, we deduce from the definition of the Euclidean minimum spanning tree that $\mathcal{G}_{\mathrm{EMST}}(C)$ is equal to the subgraph of $\mathcal{G}_{\mathrm{EMST}}(\mathcal{P})$ induced by C. Therefore, $\mathcal{G}_{\mathrm{EMST}}(C) \subset \mathcal{G}_{\mathrm{EMST}} \cap \mathcal{G}_{\mathrm{disk}}(r)(\mathcal{P})$, and p_i and

p_j belong to the same component of $\mathcal{G}_{\mathrm{EMST}} \cap \mathcal{G}_{\mathrm{disk}}(r)(\mathcal{P})$. This implies the result. ■

2.5.2 Proof of Proposition 2.9

Proof. Regarding the statement on $\mathcal{G}_{\mathrm{RN}} \cap \mathcal{G}_{\mathrm{disk}}(r)$, note that

$$B(p_i, \|p_i - p_j\|_2) \cap B(p_j, \|p_i - p_j\|_2) \subset B(p_i, \|p_i - p_j\|_2).$$

Therefore, if $\|p_i - p_j\|_2 \leq r$, then any node contained in the intersection $B(p_i, \|p_i - p_j\|_2) \cap B(p_j, \|p_i - p_j\|_2)$ must necessarily be within a distance r of p_i. From here, we deduce that $\mathcal{G}_{\mathrm{RN}} \cap \mathcal{G}_{\mathrm{disk}}(r)$ is spatially distributed over $\mathcal{G}_{\mathrm{disk}}(r)$. Regarding the statement on $\mathcal{G}_{\mathrm{G}} \cap \mathcal{G}_{\mathrm{disk}}(r)$, note that

$$B\Big(\frac{p_i + p_j}{2}, \frac{\|p_i - p_j\|_2}{2}\Big) \subset B(p_i, \|p_i - p_j\|_2).$$

Therefore, if $\|p_i - p_j\|_2 \leq r$, then any node contained in $B\big(\frac{p_i+p_j}{2}, \frac{\|p_i-p_j\|_2}{2}\big)$ must necessarily be within a distance r of p_i. From here, we deduce that $\mathcal{G}_{\mathrm{G}} \cap \mathcal{G}_{\mathrm{disk}}(r)$ is spatially distributed over $\mathcal{G}_{\mathrm{disk}}(r)$. Finally, note that if $\|p_i - p_j\|_2 > r$, then the half-plane $\{q \in \mathbb{R}^2 \mid \|q - p_i\|_2 \leq \|q - p_j\|_2\}$ contains the ball $\overline{B}(p_i, \frac{r}{2})$. Accordingly,

$$\begin{aligned} V_{i,\frac{r}{2}}(\mathcal{P}) &= V_i(\mathcal{P}) \cap \overline{B}(p_i, \tfrac{r}{2}) \\ &= \{q \in \mathbb{R}^2 \mid \|q - p_i\|_2 \leq \|q - p_j\|_2, \text{ for all } p_j \in \mathcal{P}\} \cap \overline{B}(p_i, \tfrac{r}{2}) \\ &= \{q \in \mathbb{R}^2 \mid \|q - p_i\|_2 \leq \|q - p_j\|_2, \text{ for all } p_j \in \mathcal{N}_{\mathcal{G}_{\mathrm{disk}}(r), p_i}(\mathcal{P})\} \cap \overline{B}(p_i, \tfrac{r}{2}), \end{aligned}$$

from which we deduce that $\mathcal{G}_{\mathrm{LD}}(r)$ is spatially distributed over $\mathcal{G}_{\mathrm{disk}}(r)$. ■

2.5.3 Proof of Theorem 2.16

We begin with some preliminary notions. In the following, a set $\Omega \subset \mathbb{R}^2$ is *piecewise continuously differentiable* if its boundary, $\partial\Omega$, is a not self-intersecting closed curve that admits a continuous and piecewise continuously differentiable parameterization $\gamma : [0, 1] \to \mathbb{R}^2$. Likewise, a collection of sets $\{\Omega(x) \subset \mathbb{R}^2 \mid x \in (a, b)\}$ is a *piecewise continuously differentiable family* if $\Omega(x)$ is piecewise continuously differentiable for all $x \in (a, b)$, and there exists a continuous function $\gamma : [0, 1] \times (a, b) \to \mathbb{R}^2$, $(t, x) \mapsto \gamma(t, x)$, continuously differentiable with respect to its second argument, such that for each $x \in (a, b)$, the map $t \mapsto \gamma_x(t) = \gamma(t, x)$ is a continuous and piecewise continuously differentiable parameterization of $\partial\Omega(x)$. We refer to γ as a *parameterization for the family* $\{\Omega(x) \subset \mathbb{R}^2 \mid x \in (a, b)\}$.

The following result is an extension of the Law of Conservation of Mass in fluid mechanics (Chorin and Marsden, 1994) and of the classic divergence theorem in differential geometry (Chavel, 1984).

Proposition 2.23 (Generalized conservation of mass). *Let $\{\Omega(x) \subset \mathbb{R}^2 \mid x \in (a,b)\}$ be a family of star-shaped sets with piecewise continuously differentiable boundary. Let the function $\phi : \mathbb{R}^2 \times (a,b) \to \mathbb{R}$ be continuous on $\mathbb{R}^2 \times (a,b)$ that is continuously differentiable with respect to its second argument for all $x \in (a,b)$ and almost all $q \in \Omega(x)$, and such that for each $x \in (a,b)$, the maps $q \mapsto \phi(q,x)$ and $q \mapsto \frac{\partial \phi}{\partial x}(q,x)$ are measurable, and integrable on $\Omega(x)$. Then, the function*

$$(a,b) \ni x \mapsto \int_{\Omega(x)} \phi(q,x) dq \tag{2.5.1}$$

is continuously differentiable and

$$\frac{d}{dx} \int_{\Omega(x)} \phi(q,x) dq = \int_{\Omega(x)} \frac{\partial \phi}{\partial x}(q,x) dq + \int_{\partial\Omega(x)} \phi(\gamma,x) \Big(n(\gamma) \cdot \frac{\partial \gamma}{\partial x} \Big) d\gamma \,,$$

where $n : \partial\Omega(x) \to \mathbb{R}^2$, $q \mapsto n(q)$, denotes the unit outward normal to $\partial\Omega(x)$ at $q \in \partial\Omega(x)$, and $\gamma : [0,1] \times (a,b) \to \mathbb{R}^2$ is a parameterization for the family $\{\Omega(x) \subset \mathbb{R}^2 \mid x \in (a,b)\}$.

We interpret the proposition as follows: in the fluid mechanics interpretation, as the parameter x changes, the total mass variation inside the region can be decomposed into two terms. The first term is the amount of mass created inside the region, whereas the second term is the amount of mass that crosses the moving boundary of the region.

Proof of Proposition 2.23. Let $x_0 \in (a,b)$. Using the fact that the map γ is continuous and that $\Omega(x_0)$ is star-shaped, one can show that there exist an interval around x_0 of the form $(x_0 - \varepsilon, x_0 + \varepsilon)$, a continuously differentiable function $u_{x_0} : [0,1] \times \mathbb{R}_{\geq 0} \to \mathbb{R}^2$ and a function $r_{x_0} : [0,1] \times (x_0 - \varepsilon, x_0 + \varepsilon) \to \mathbb{R}_{\geq 0}$ continuously differentiable in its second argument and piecewise continuously differentiable in its first argument, such that for all $x \in (x_0 - \varepsilon, x_0 + \varepsilon)$, one has

$$\begin{aligned} \Omega(x) &= \cup_{t \in [0,1]} \{ u_{x_0}(t,s) \mid 0 \leq s \leq r_{x_0}(t,x) \}, \\ \gamma(t,x) &= u_{x_0}(t, r_{x_0}(t,x)), \quad \text{for all } t \in [0,1]. \end{aligned}$$

For simplicity, we denote by r and u the functions r_{x_0} and u_{x_0}, respectively. By definition, the function in (2.5.1) is continuously differentiable at x_0 if the following limit exists:

$$\lim_{h \to 0} \frac{1}{h} \Big(\int_{\Omega(x_0+h)} \phi(q, x_0 + h) dq - \int_{\Omega(x_0)} \phi(q, x_0) dq \Big),$$

and depends continuously on x_0. Now, we can rewrite the previous limit as

$$\begin{aligned}
\lim_{h\to 0}\frac{1}{h}\int_0^1 \Big(\int_0^{r(t,x_0+h)} & \phi(u(t,s),x_0+h)\Big\|\frac{\partial u}{\partial t}\times\frac{\partial u}{\partial s}\Big\|_2 ds \\
& - \int_0^{r(t,x_0)} \phi(u(t,s),x_0)\Big\|\frac{\partial u}{\partial t}\times\frac{\partial u}{\partial s}\Big\|_2 ds\Big) dt \\
= \lim_{h\to 0}\frac{1}{h}\int_0^1 \Big(\int_{r(t,x_0)}^{r(t,x_0+h)} & \phi(u(t,s),x_0+h)\Big\|\frac{\partial u}{\partial t}\times\frac{\partial u}{\partial s}\Big\|_2 ds \\
+ \int_0^{r(t,x_0)} & (\phi(u(t,s),x_0+h)-\phi(u(t,s),x_0))\Big\|\frac{\partial u}{\partial t}\times\frac{\partial u}{\partial s}\Big\|_2 ds\Big) dt, \quad (2.5.2)
\end{aligned}$$

where $\times$ denotes the vector product and for brevity we omit the fact that the partial derivatives $\frac{\partial u}{\partial t}$ and $\frac{\partial u}{\partial s}$ are evaluated at (t,s) in the integrals. Regarding the second integral in the last equality of (2.5.2), since

$$\begin{aligned}
\lim_{h\to 0}\frac{1}{h}\Big((\phi(u(t,s),x_0+h)-\phi(u(t,s),x_0))\Big\|\frac{\partial u}{\partial t}\times\frac{\partial u}{\partial s}\Big\|_2\Big) & \\
= \frac{\partial\phi}{\partial x_0}(u(t,s),x_0)\Big\|\frac{\partial u}{\partial t}\times\frac{\partial u}{\partial s}\Big\|_2, &
\end{aligned}$$

almost everywhere, and this function is measurable and its integral over the bounded set $\Omega(x_0)$ is finite by hypothesis, the Lebesgue Dominated Convergence Theorem (Bartle, 1995) implies that

$$\begin{aligned}
\lim_{h\to 0}\frac{1}{h}\int_0^1\int_0^{r(t,x_0)} & (\phi(u(t,s),x_0+h)-\phi(u(t,s),x_0))\Big\|\frac{\partial u}{\partial t}\times\frac{\partial u}{\partial s}\Big\|_2 ds dt \\
&= \int_0^1\int_0^{r(t,x_0)} \frac{\partial\phi}{\partial x}(u(t,s),x_0)\Big\|\frac{\partial u}{\partial t}\times\frac{\partial u}{\partial s}\Big\|_2 ds dt \\
&= \int_{\Omega(x_0)} \frac{\partial\phi}{\partial x}(q,x_0)dq. \quad (2.5.3)
\end{aligned}$$

On the other hand, regarding the first integral in the last equality of (2.5.2), using the continuity of ϕ, one can deduce that

$$\begin{aligned}
\lim_{h\to 0}\frac{1}{h}\int_0^1\int_{r(t,x_0)}^{r(t,x_0+h)} & \phi(u(t,s),x_0+h)\Big\|\frac{\partial u}{\partial t}(t,s)\times\frac{\partial u}{\partial s}(t,s)\Big\|_2 ds\, dt \\
= \lim_{h\to 0}\frac{1}{h}\int_0^1\int_{x_0}^{x_0+h} & \phi(u(t,r(t,z)),x_0+h) \\
& \cdot\Big\|\frac{\partial u}{\partial t}(t,r(t,z))\times\frac{\partial u}{\partial s}(t,r(t,z))\Big\|_2\frac{\partial r}{\partial x}(t,z)\, dz\, dt \\
= \int_0^1 & \phi(u(t,r(t,x_0)),x_0)\Big\|\frac{\partial u}{\partial t}(t,r(t,x_0))\times\frac{\partial u}{\partial s}(t,r(t,x_0))\Big\|_2\frac{\partial r}{\partial x_0}(t,x_0)\, dt.
\end{aligned}$$

Since $\gamma(t,x) = u(t, r(t,x))$ for all $t \in [0,1]$ and $x \in (x_0 - \varepsilon, x_0 + \varepsilon)$, one has

$$\frac{\partial \gamma}{\partial t}(t,x_0) = \frac{\partial u}{\partial t}(t, r(t,x_0)) + \frac{\partial u}{\partial s}(t, r(t,x_0))\frac{\partial r}{\partial t}(t,x_0)\,,$$
$$\frac{\partial \gamma}{\partial x}(t,x_0) = \frac{\partial u}{\partial s}(t, r(t,x_0))\frac{\partial r}{\partial x}(t,x_0).$$

Let χ denote the angle formed by $\frac{\partial \gamma}{\partial t}(t,x_0)$ and $\frac{\partial u}{\partial s}(t, r(t,x_0))$. Then (omitting the expression $(t, r(t,x))$ for brevity),

$$\begin{aligned}\left\|\frac{\partial u}{\partial t} \times \frac{\partial u}{\partial s}\right\|_2 &= \left\| \left(\frac{\partial u}{\partial t} + \frac{\partial u}{\partial s}\frac{\partial r}{\partial t}\right) \times \frac{\partial u}{\partial s}\right\|_2 \\ &= \left\|\frac{d\gamma}{dt}\right\|_2 \left\|\frac{\partial u}{\partial s}\right\|_2 \sin\chi = \left\|\frac{\partial \gamma}{\partial t}\right\|_2 n^T(\gamma)\frac{\partial u}{\partial s},\end{aligned}$$

where in the last inequality we have used the fact that, since γ_{x_0} is a parameterization of $\partial\Omega(x_0)$, then $\sin\chi = \cos\psi$, where ψ is the angle formed by n, the outward normal to $\partial\Omega(x_0)$, and $\frac{\partial u}{\partial s}$. Therefore, we finally arrive at

$$\begin{aligned}\int_0^1 \phi(\gamma(t), x_0) &\left\|\frac{\partial u}{\partial t}(t, r(t,x_0)) \times \frac{\partial u}{\partial s}(t, r(t,x_0))\right\|_2 \frac{\partial r}{\partial x}(t,x_0)dt \\ &= \int_0^1 \phi(\gamma(t), x_0)\left\|\frac{\partial \gamma}{\partial t}(t,x_0)\right\|_2 n^T(\gamma(t,x_0))\frac{\partial \gamma}{\partial x}(t,x_0)dt \\ &= \int_{\partial\Omega(x_0)} \phi(\gamma, x_0) n^T(\gamma)\frac{\partial \gamma}{\partial x}d\gamma. \qquad (2.5.4)\end{aligned}$$

Given the hypothesis of Proposition 2.23, both terms in (2.5.3) and (2.5.4) have a continuous dependence on $x_0 \in (a,b)$. This concludes the proof. ■

We are finally ready to state the proof of the main result of Section 2.3.

Proof of Theorem 2.16. We prove the theorem statement when the performance function is continuously differentiable and we refer to Cortés et al. (2005) for the complete proof for the case when the performance function is piecewise continuously differentiable. Specifically, we show that if f is continuously differentiable, then for $P \in S^n \setminus \mathcal{S}_{\text{coinc}}$,

$$\frac{\partial \mathcal{H}_{\text{exp}}}{\partial p_i}(P) = \int_{V_i(\mathcal{P})} \frac{\partial}{\partial p_i} f(\|q - p_i\|_2)\phi(q)dq.$$

From Proposition 2.23, we have

$$\frac{\partial}{\partial p_i}\Big(\sum_{j=1}^{n}\int_{V_j(\mathcal{P})} f(\|q-p_j\|_2)\phi(q)dq\Big) = \int_{V_i(\mathcal{P})}\frac{\partial}{\partial p_i} f(\|q-p_i\|_2)\phi(q)dq + \sum_{j=1}^{n}\int_{\partial V_j(\mathcal{P})}\varphi(p_j,q)\Big(n(\gamma_j)\cdot\frac{\partial\gamma_j}{\partial p_i}\Big)d\gamma_j,$$

where γ_j is a parametrization of $V_j(\mathcal{P})$ and where we abbreviate $\varphi(p_j,q) = f(\|q-p_j\|_2)\phi(q)$. Next, we show that the second term vanishes. Note that the motion of p_i affects the Voronoi cell $V_i(\mathcal{P})$ and the cells of all its neighbors in $\mathcal{N}_{\mathcal{G}_{\mathrm{D}},p_i}(\mathcal{P})$. Therefore, the second term equals

$$\int_{\partial V_i(\mathcal{P})}\varphi(p_i,q)\Big(n(\gamma_i)\cdot\frac{\partial\gamma_i}{\partial p_i}\Big)d\gamma_i + \sum_{p_j\in\mathcal{N}_{\mathcal{G}_{\mathrm{D}},p_i}(\mathcal{P})}\int_{\partial V_j(\mathcal{P})}\varphi(p_j,q)\Big(n(\gamma_j)\cdot\frac{\partial\gamma_j}{\partial p_i}\Big)d\gamma_j.$$

Without loss of generality, assume that $V_i(\mathcal{P})$ does not share any face with ∂S. Since the boundary of $V_i(\mathcal{P})$ satisfies $\partial V_i(\mathcal{P}) = \bigcup_j \Delta_{ij}$, where $\Delta_{ij} = \Delta_{ji}$ is the edge between $V_i(\mathcal{P})$ and $V_j(\mathcal{P})$, for all neighbors p_j, we compute

$$\int_{\partial V_i(\mathcal{P})}\varphi(p_i,q)\Big(n(\gamma_i)\cdot\frac{\partial\gamma_i}{\partial p_i}\Big)d\gamma_i = \sum_{p_j\in\mathcal{N}_{\mathcal{G}_{\mathrm{D}},p_i}(\mathcal{P})}\int_{\Delta_{ij}}\varphi(p_i,q)\Big(n_{ij}(\gamma_j)\cdot\frac{\partial\gamma_j}{\partial p_i}\Big)d\gamma_j,$$

$$\int_{\partial V_j(\mathcal{P})}\varphi(p_j,q)\Big(n(\gamma_j)\cdot\frac{\partial\gamma_j}{\partial p_i}\Big)d\gamma_j = \int_{\Delta_{ji}}\varphi(p_j,q)\Big(n_{ji}(\gamma_j)\cdot\frac{\partial\gamma_j}{\partial p_i}\Big)d\gamma_j,$$

where n_{ij} denotes the unit normal along Δ_{ij} outward of $V_i(P)$. Noting that $n_{ji} = -n_{ij}$ and collecting the results obtained so far, we write

$$\sum_{j=1}^{n}\int_{\partial V_j(\mathcal{P})}\varphi(p_j,q)\Big(n(\gamma_j)\cdot\frac{\partial\gamma_j}{\partial p_i}\Big)d\gamma_j = \sum_{p_j\in\mathcal{N}_{\mathcal{G}_{\mathrm{D}},p_i}(\mathcal{P})}\int_{\Delta_{ij}}\Big(\varphi(p_i,q)-\varphi(p_j,q)\Big)\Big(n_{ij}(\gamma_j)\cdot\frac{\partial\gamma_j}{\partial p_i}\Big)d\gamma_j.$$

This quantity vanishes because $f(\|q-p_i\|_2) = f(\|q-p_j\|_2)$, and therefore $\varphi(p_i,q) = \varphi(p_j,q)$ for any q belonging to the edge Δ_{ij}. ■

2.5.4 Proof of Proposition 2.19

Proof. Recall that $\mathcal{H}_{\mathrm{dc}}(p_1,\dots,p_n) = \mathcal{H}_{\mathrm{dc}}(p_1,\dots,p_n,V_1(\mathcal{P}),\dots,V_n(\mathcal{P}))$. To show the first inequality, let $j\in\{1,\dots,n\}$ and $q_*\in V_j(\mathcal{P})$ be such that

$\mathcal{H}_{\mathrm{dc}}(p_1, \dots, p_n) = \|q_* - p_j\|_2$. By definition, given a partition $\{W_1, \dots, W_n\}$ of S, there exists k such that $q_* \in W_k$. Therefore,

$$\begin{aligned}\mathcal{H}_{\mathrm{dc}}(p_1, \dots, p_n) &= \|q_* - p_j\|_2 \leq \|q_* - p_k\|_2 \\ &\leq \max_{q \in W_k} \|q - p_j\|_2 \leq \mathcal{H}_{\mathrm{dc}}(p_1, \dots, p_n, W_1, \dots, W_n).\end{aligned}$$

To show the second inequality, note that the definition of circumcenter implies that, for each $i \in \{1, \dots, n\}$,

$$\max_{q \in \partial W_i} \|q - \mathrm{CC}(W_i)\|_2 \leq \max_{q \in \partial W_i} \|q - p_i\|_2.$$

Taking the maximum over all nodes, we deduce that

$$\mathcal{H}_{\mathrm{dc}}(\mathrm{CC}(W_1), \dots, \mathrm{CC}(W_n), W_1, \dots, W_n) \leq \mathcal{H}_{\mathrm{dc}}(p_1, \dots, p_n, W_1, \dots, W_n),$$

as claimed. ■

2.5.5 Proof of Proposition 2.21

Proof. Recall that $\mathcal{H}_{\mathrm{sp}}(p_1, \dots, p_n) = \mathcal{H}_{\mathrm{sp}}(p_1, \dots, p_n, V_1(\mathcal{P}), \dots, V_n(\mathcal{P}))$. To show the first inequality, let $j \in \{1, \dots, n\}$ and $q_* \notin \mathrm{int}(V_j(\mathcal{P}))$ be such that $\mathcal{H}_{\mathrm{sp}}(p_1, \dots, p_n) = \|q_* - p_j\|_2$. Since $q_* \notin \mathrm{int}(V_j(\mathcal{P}))$, there exists $i \in \{1, \dots, n\}$ such that $\|q_* - p_j\|_2 \geq \|q_* - p_i\|_2$. On the other hand, there must exist $k \in \{1, \dots, n\}$ such that $q_* \in W_k$. Now, if $k = j$, then $q_* \notin \mathrm{int}(W_i)$. Therefore,

$$\begin{aligned}\mathcal{H}_{\mathrm{sp}}(p_1, \dots, p_n) &= \|q_* - p_j\|_2 \geq \|q_* - p_i\|_2 \\ &\geq \min_{q \notin \mathrm{int}(W_i)} \|q - p_i\|_2 \geq \mathcal{H}_{\mathrm{sp}}(p_1, \dots, p_n, W_1, \dots, W_n).\end{aligned}$$

Now, if $k = i$, then $q_* \notin \mathrm{int}(W_j)$. Therefore,

$$\mathcal{H}_{\mathrm{sp}}(P) = \|q_* - p_j\|_2 \geq \min_{q \notin \mathrm{int}(W_j)} \|q - p_i\|_2 \geq \mathcal{H}_{\mathrm{sp}}(p_1, \dots, p_n, W_1, \dots, W_n).$$

Finally, if $k \neq i, j$, then $q_* \notin \mathrm{int}(W_i) \cup \mathrm{int}(W_j)$, and a similar argument guarantees $\mathcal{H}_{\mathrm{sp}}(p_1, \dots, p_n) \geq \mathcal{H}_{\mathrm{sp}}(p_1, \dots, p_n, W_1, \dots, W_n)$.

To show the second inequality, let $i \in \{1, \dots, n\}$ and select $q_i \in \mathrm{IC}(W_i)$. The definition of the incenter set implies that,

$$\min_{q \in \partial W_i} \|q - q_i\|_2 \geq \min_{q \in \partial W_i} \|q - p_i\|_2.$$

The expression on the left does not depend on the specific point selected in the incenter set. Taking the minimum over all nodes, we deduce that

$$\mathcal{H}_{\mathrm{sp}}(\mathrm{IC}(W_1), \dots, \mathrm{IC}(W_n), W_1, \dots, W_n) \geq \mathcal{H}_{\mathrm{sp}}(p_1, \dots, p_n, W_1, \dots, W_n),$$

as claimed. ■

2.6 EXERCISES

E2.1 **(Proof of Lemma 2.2).** For $S = \{p_1, \ldots, p_n\} \in \mathbb{F}(\mathbb{R}^d)$ with $n \geq 2$, prove the following statements:

(i) $\mathrm{CC}(S) \in \mathrm{co}(S) \setminus \mathrm{Ve}(\mathrm{co}(S))$;

(ii) if $p \in \mathrm{co}(S) \setminus \{\mathrm{CC}(S)\}$ and $r \in \mathbb{R}_{>0}$ are such that $S \subset \overline{B}(p, r)$, then the segment $]p, \mathrm{CC}(S)[$ has a nonempty intersection with $\overline{B}(\frac{p+q}{2}, \frac{r}{2})$ for all $q \in \mathrm{co}(S)$.

Hint: *To show (i), invoke the definition of circumcenter. To show (ii), distinguish between the case when $\|p-q\|_2 < r$ and $\|p-q\|_2 = r$. A proof is contained in Cortés et al. (2006).*

E2.2 **(The centroid of a convex set is an interior point).** Let S be a bounded measurable convex set in $\mathbb{R}^d$ and let $\phi : S \to \mathbb{R}_{>0}$ be a bounded measurable density function that is positive over S. Show that

$$\mathrm{CM}_\phi(S) \in \mathrm{int}(S).$$

E2.3 **(The inclusion $\mathcal{G}_{\mathbf{LD}}(r) \subset \mathcal{G}_{\mathbf{D}} \cap \mathcal{G}_{\mathbf{disk}}(r)$ is in general strict).** Consider the nodes $p_1 = (0, 0)$, $p_2 = (1, 0)$, and $p_3 = (2, \frac{1}{10})$. Pick $r = 3$ and perform the following tasks:

(i) draw the three points, their Voronoi polygons and the disks centered at the points with radius r; and

(ii) show that p_1 and p_3 are neighbors in the graph $\mathcal{G}_{\mathrm{D}} \cap \mathcal{G}_{\mathrm{disk}}(r)$, but not in the graph $\mathcal{G}_{\mathrm{LD}}(r)$.

E2.4 **(The proximity graph $\mathcal{G}_{\mathbf{D}} \cap \mathcal{G}_{\mathbf{disk}}(r)$ is not spatially distributed over $\mathcal{G}_{\mathbf{disk}}(r)$).** Consider the nodes $p_1 = (0, 0)$, $p_2 = (1, 0)$, $p_3 = (2, \frac{1}{10})$, and $p_4 = (0, \frac{31}{10})$. Compute the Voronoi partitions of the plane generated by $\{p_1, p_2.p_3\}$ and $\{p_1, p_2, p_3, p_4\}$. For $r = 3$, show that p_1 and p_3 are neighbors in the graph $\mathcal{G}_{\mathrm{D}} \cap \mathcal{G}_{\mathrm{disk}}(r)(\{p_1, p_2, p_3\})$ but not in the graph $\mathcal{G}_{\mathrm{D}} \cap \mathcal{G}_{\mathrm{disk}}(r)(\{p_1, p_2, p_3, p_4\})$. Why does this exercise illustrate that $\mathcal{G}_{\mathrm{D}} \cap \mathcal{G}_{\mathrm{disk}}(r)$ is not spatially distributed over $\mathcal{G}_{\mathrm{disk}}(r)$?

E2.5 **(1-center area problem).** Let $W \subset \mathbb{R}^2$ be a convex polygon, let ϕ be a density function on $\mathbb{R}^2$, and let $a \in \mathbb{R}_{>0}$. Assume that the a-contraction of W is nonempty. Consider the area function $\mathcal{H}_1 : W \to \mathbb{R}$, defined by

$$\mathcal{H}_1(p) = \int_{W \cap \overline{B}(p,a)} \phi(q) dq = \mathrm{A}_\phi(W \cap \overline{B}(p, a)).$$

Justify informally why, at points in the boundary of a convex polygon W, the gradient of $\mathcal{H}_1$ is non-vanishing, and points toward the interior of the polygon. (Note that it is not known whether the function $\mathcal{H}_1$ is concave and how to characterize critical points of $\mathcal{H}_1$ in geometric terms.)

E2.6 **(Concavity of performance function and 1-center function).** Given a performance function f, define the 1-center function $\mathcal{H}_{\mathrm{exp},1} : S \to \mathbb{R}$ by

$$\mathcal{H}_{\mathrm{exp},1}(p) = \int_S f(\|q - p\|_2)\phi(q) dq.$$

Prove the following facts:

(i) if f is concave, then $\mathcal{H}_{\text{exp},1}$ is concave; and

(ii) if f is concave and decreasing and S has positive measure, then $\mathcal{H}_{\text{exp},1}$ is strictly concave.

E2.7 **(Fermat–Weber center).** Let $S \subset \mathbb{R}^2$ be a convex polygon and let ϕ be a density function on S. Define the *Fermat–Weber function* $\mathcal{H}_{\text{FW}} : \mathbb{R}^2 \to \mathbb{R}$ by

$$\mathcal{H}_{\text{FW}}(p) = \int_S \|p - q\|_2 \phi(q) dq.$$

(i) Prove that $\mathcal{H}_{\text{FW}}$ is strictly convex.

(ii) Show that $\mathcal{H}_{\text{FW}}$ has a unique global minimum point inside S.

(iii) Compute the derivative of $\mathcal{H}_{\text{FW}}$ and propose an algorithm to compute the global minimum point.

(iv) Is the function strictly convex even if the polygon S is not convex?

The unique minimum of $\mathcal{H}_{\text{FW}}$ is called the *Fermat–Weber point* or, alternatively, the *median point* of the region S. Further details on this problem are available in Fekete et al. (2005) and references therein.

E2.8 **(Proof of Proposition 2.14).** In this exercise, you are asked to prove a statement that is slightly more general than Proposition 2.14. Let $\{W_1, \ldots, W_n\} \subset \mathbb{P}(S)$ be a partition of $S \subset \mathbb{R}^d$ and let ϕ be a density function on $\mathbb{R}^d$. Select $\{p_1, \ldots, p_n\}, \{\overline{p}_1, \ldots, \overline{p}_n\} \in \mathbb{F}(S)$ with the property that, for all $i \in \{1, \ldots, n\}$,

$$\|\overline{p}_i - \text{CM}_\phi(W_i)\|_2 \leq \|p_i - \text{CM}_\phi(W_i)\|_2.$$

Show that

$$\mathcal{H}_{\text{dist}}(\overline{p}_1, \ldots, \overline{p}_n, W_1, \ldots, W_n) \geq \mathcal{H}_{\text{dist}}(p_1, \ldots, p_n, W_1, \ldots, W_n),$$

and that the inequality is strict if there exists $i \in \{1, \ldots, n\}$ such that $\|\overline{p}_i - \text{CM}_\phi(W_i)\|_2 < \|p_i - \text{CM}_\phi(W_i)\|_2$ and such that W_i has positive area.
Hint: *Use the expression of* $\mathcal{H}_{\text{dist}}$ *in* (2.3.5).

E2.9 **(Mixed distortion-area multicenter function).** Show that the expected multicenter function $\mathcal{H}_{\text{exp}}$ takes the form of $\mathcal{H}_{\text{dist-area},a,b}$ stated in Section 2.3.1 when the performance function is

$$f(x) = -x^2 \, 1_{[0,a]}(x) + b \cdot 1_{]a,+\infty[}(x),$$

with $a \in \mathbb{R}_{>0}$ and $b \leq -a^2$.
Hint: *As an intermediate step, show that for* $P = (p_1, \ldots, p_n) \in S^n$, *one has* $V_i(P) \cap (S \setminus \overline{B}(p_i, a)) = V_i(P) \cap \left(S \setminus \cup_{k=1}^n \overline{B}(p_k, a)\right)$ *for all* $i \in \{1, \ldots, n\}$.

E2.10 **(Proof of Proposition 2.15).** This exercise is a guided proof of Proposition 2.15. Let $W \subset \mathbb{R}^d$ be a connected set, let ϕ be a density function on $\mathbb{R}^d$, and let $a \in \mathbb{R}_{>0}$. For $p \in W$ and $\overline{B}$ a closed ball centered at a point in W with radius a, define $(p, \overline{B}) \mapsto \mathcal{H}_W(p, \overline{B})$ by

$$\mathcal{H}_W(p, \overline{B}) = -\int_{W \cap \overline{B}} \|q - p\|_2^2 \phi(q) dq - \int_{W \cap (S \setminus \overline{B})} a^2 \phi(q) dq.$$

Do the following:

(i) Show that the multicenter function $\mathcal{H}_{\text{dist-area},a}$ admits the expression

$$\mathcal{H}_{\text{dist-area},a}(p_1,\dots,p_n,W_1,\dots,W_n)=\sum_{i=1}^{n}\mathcal{H}_{W_i}(p_i,\overline{B}(p_i,a)).$$

(ii) Given a closed ball $\overline{B}$ centered at a point in W with radius a, show that for any $p\in W$,

$$\mathcal{H}_W(\text{CM}_\phi(W\cap\overline{B}),\overline{B})\geq\mathcal{H}_W(p,\overline{B}),$$

with strict inequality unless $p=\text{CM}_\phi(W\cap\overline{B})$.
Hint: *Use the Parallel Axis Theorem (Hibbeler, 2006).*

(iii) Given $p\in W$, show that for any closed ball $\overline{B}$ centered at a point in W with radius a,

$$\mathcal{H}_W(p,\overline{B}(p,a))\geq\mathcal{H}_W(p,\overline{B}).$$

Hint: *Consider the decomposition of W given by the union of the disjoint sets $\overline{B}(p,a)\cap\overline{B}$, $\overline{B}(p,a)\cap(W\setminus\overline{B})$, $(W\setminus\overline{B}(p,a))\cap\overline{B}$ and $(W\setminus\overline{B}(p,a))\cap(W\setminus\overline{B})$, and compare the integrals over each set.*

(iv) Deduce, using (ii) and (iii), that

$$\mathcal{H}_W(\text{CM}_\phi(W\cap\overline{B}(p,a)),\overline{B}(\text{CM}_\phi(W\cap\overline{B}(p,a)),a))\geq\mathcal{H}_W(p,\overline{B}(p,a)),$$

with strict inequality unless $p=\text{CM}_\phi(W\cap\overline{B})$.

(v) Combine (i) and (iv) to prove Proposition 2.15.

E2.11 **(Locally cliqueless proximity graph).** Give an example of an allowable environment Q and a configuration of points such that the following inclusions (taken from Theorem 2.11(i)) are strict for $\mathcal{G}=\mathcal{G}_{\text{vis},Q}$:

$$\mathcal{G}_{\text{EMST},\mathcal{G}}\subseteq\mathcal{G}_{\text{lc},\mathcal{G}}\subseteq\mathcal{G},$$

E2.12 **(Properties of the locally cliqueless graph).** Prove Theorem 2.11.
Hint: *This exercise has notable theoretical content. To prove Theorem 2.11(i), use an argument by contradiction to show that the first inclusion holds, and use the definition of locally cliqueless graph to show that the second inclusion holds.*

E2.13 **(When are the total derivative and the partial derivative of a function equal?).** Assume that $f:\mathbb{R}\times\mathbb{R}\to\mathbb{R}$ is continuously differentiable in its both of its arguments and let $\partial_1 f$ be its partial derivative with respect to its first argument. Assume that the function $y^*:\mathbb{R}\to\mathbb{R}$ satisfies, for each $x\in\mathbb{R}$,

$$f(x,y^*(x))=\max\{f(x,z)\mid z\in\mathbb{R}\},$$

and is continuously differentiable. Perform the following tasks:

(i) Show that

$$\frac{d}{dx}f(x,y^*(x))=\partial_1 f(x,y^*(x)).\tag{E2.1}$$

(ii) Explain how this result gives an insight into the expression of the gradient of $\mathcal{H}_{\text{exp}}$ in Theorem 2.16(ii) for a continuously differentiable performance function. Also, explain why this formula is not directly applicable to the function $\mathcal{H}_{\text{exp}}$.

Note that equation (E2.1) is referred to as the *envelope theorem* in the economics literature.

E2.14 **(Distortion gradient ascent flow).** Given a (convex) polytope $S \subset \mathbb{R}^d$ and a density function ϕ, consider n nodes $p_1, \dots, p_n$ evolving under the continuous-time gradient ascent flow of the multicenter function $\mathcal{H}_{\text{dist}}$,

$$\dot{p}_i = 2\,\mathrm{A}_\phi(V_i(\mathcal{P}))(\mathrm{CM}_\phi(V_i(\mathcal{P})) - p_i), \quad i \in \{1, \dots, n\}.$$

(i) What are the equilibrium points?

(ii) Show that $\mathcal{H}_{\text{dist}}$ is monotonically non-decreasing along the flow.

(iii) Show that the set S^N is invariant, i.e., that the trajectories of all nodes remain in S.

(iv) Use (i)–(iii) to apply the LaSalle Invariance Principle and show that the solutions of the flow converge to the set of centroidal Voronoi configurations in S.

(v) Implement numerically the flow in the software of your choice. Select the unit square $S = [0,1] \times [0,1]$ and the density function

$$\phi = \exp\Big(-\big(x - \frac{1}{8}\big)^2 - \big(y - \frac{1}{8}\big)^2\Big) + \exp\Big(-\big(x - \frac{7}{8}\big)^2 - \big(y - \frac{7}{8}\big)^2\Big).$$

Run simulations from different initial conditions and with different numbers of nodes. Show by illustration that multiple local maxima exist.

Hint: *To perform step (iv), one should also prove that any two nodes never converge to the same location (in finite or infinite time); this property needs to be established because the function $\mathcal{H}_{\text{dist}}$ is not differentiable on such configurations. For this and the next exercise, do not worry about proving this property and instead refer to Cortés et al. (2005, Proposition 3.1).*

E2.15 **(Area gradient ascent flow).** Given a (convex) polytope $S \subset \mathbb{R}^d$, a density function ϕ, and a radius $a \in \mathbb{R}_{>0}$, consider n nodes $p_1, \dots, p_n$ evolving under the continuous-time gradient ascent flow of the multicenter function $\mathcal{H}_{\text{area},a}$,

$$\dot{p}_i = \int_{V_i(\mathcal{P}) \cap \partial\overline{B}(p_i,a)} \mathrm{n}_{\text{out}}(q)\phi(q)dq, \quad i \in \{1, \dots, n\},$$

where n_{out} is the outward normal vector to the ball $\overline{B}(p_i, a)$.

(i) What are the equilibrium points?

(ii) Show that $\mathcal{H}_{\text{area},a}$ is monotonically non-decreasing along the flow.

(iii) Show that the set S^N is invariant, i.e., that the trajectories of all nodes remain in S.

(iv) Use (i-)-(iii) to apply the LaSalle Invariance Principle and show that the solutions of the flow converge to the set of a-limited area-centered Voronoi configurations in S.

(v) Implement numerically the flow in the software of your choice. Select the unit square $S = [0,1] \times [0,1]$, the density function

$$\phi(x,y) = \exp\Big(-\big(x - \frac{1}{8}\big)^2 - \big(y - \frac{1}{8}\big)^2\Big) + \exp\Big(-\big(x - \frac{7}{8}\big)^2 - \big(y - \frac{7}{8}\big)^2\Big),$$

and the parameter $a = \frac{1}{8}$. Run simulations from different initial conditions and with different numbers of nodes. Show by illustration that multiple local maxima exist.

Bibliography

Agarwal, P. K. and Sharir, M. [1998] *Efficient algorithms for geometric optimization*, ACM Computing Surveys, **30**(4), 412–458.

Aurenhammer, F. [1991] *Voronoi diagrams: A survey of a fundamental geometric data structure*, ACM Computing Surveys, **23**(3), 345–405.

Bartle, R. G. [1995] *The Elements of Integration and Lebesgue Measure*, Wiley-Interscience, ISBN 0471042226.

Boissonnat, J.-D. and Cazals, F. [2002] *Smooth surface reconstruction via natural neighbour interpolation of distance functions*, Computational Geometry: Theory and Applications, **22**(1), 185–203.

Bollobás, B. and Riordan, O. [2006] *Percolation*, Cambridge University Press, ISBN 0521872324.

Boltyanski, V., Martini, H., and Soltan, V. [1999] *Geometric methods and optimization problems*, volume 4 of *Combinatorial optimization*, Kluwer Academic Publishers, ISBN 0792354540.

Chavel, I. [1984] *Eigenvalues in Riemannian Geometry*, Academic Press, ISBN 0121706400.

Chorin, A. J. and Marsden, J. E. [1994] *A Mathematical Introduction to Fluid Mechanics*, volume 4 of *Texts in Applied Mathematics*, third edition, Springer, ISBN 0387979182.

Clarke, F. H. [1983] *Optimization and Nonsmooth Analysis*, Canadian Mathematical Society Series of Monographs and Advanced Texts, John Wiley, ISBN 047187504X.

Cortés, J. and Bullo, F. [2005] *Coordination and geometric optimization via distributed dynamical systems*, SIAM Journal on Control and Optimization, **44**(5), 1543–1574.

Cortés, J., Martínez, S., and Bullo, F. [2005] *Spatially-distributed coverage optimization and control with limited-range interactions*, ESAIM: Control, Optimisation & Calculus of Variations, **11**, 691–719.

— [2006] *Robust rendezvous for mobile autonomous agents via proximity graphs in arbitrary dimensions*, IEEE Transactions on Automatic Control, **51**(8), 1289–1298.

Cortés, J., Martínez, S., Karatas, T., and Bullo, F. [2004] *Coverage control for mobile sensing networks*, IEEE Transactions on Robotics and Automation, **20**(2), 243–255.

de Berg, M., van Kreveld, M., Overmars, M., and Schwarzkopf, O. [2000] *Computational Geometry: Algorithms and Applications*, second edition, Springer, ISBN 3540656200.

Drezner, Z., (editor) [1995] *Facility Location: A Survey of Applications and Methods*, Series in Operations Research, Springer, ISBN 0-387-94545-8.

Drezner, Z. and Hamacher, H. W., (editors) [2001] *Facility Location: Applications and Theory*, Springer, ISBN 3540421726.

Du, Q., Faber, V., and Gunzburger, M. [1999] *Centroidal Voronoi tessellations: Applications and algorithms*, SIAM Review, **41**(4), 637–676.

Fekete, S. P., Mitchell, J. S. B., and Beurer, K. [2005] *On the continuous Fermat–Weber problem*, Operations Research, **53**(1), 61 – 76.

Ganguli, A., Cortés, J., and Bullo, F. [2009] *Multirobot rendezvous with visibility sensors in nonconvex environments*, IEEE Transactions on Robotics, **25**(2), 340–352.

Goodman, J. E. and O'Rourke, J., (editors) [2004] *Handbook of Discrete and Computational Geometry*, second edition, CRC Press, ISBN 1584883014.

Gray, R. M. and Neuhoff, D. L. [1998] *Quantization*, IEEE Transactions on Information Theory, **44**(6), 2325–2383, Commemorative Issue 1948-1998.

Hibbeler, R. C. [2006] *Engineering Mechanics: Statics & Dynamics*, 11th edition, Prentice Hall, ISBN 0132215098.

Jaromczyk, J. W. and Toussaint, G. T. [1992] *Relative neighborhood graphs and their relatives*, Proceedings of the IEEE, **80**(9), 1502–1517.

Langetepe, E. and Zachmann, G. [2006] *Geometric Data Structures for Computer Graphics*, A. K. Peters, ISBN 1568812353.

Martínez, S., Cortés, J., and Bullo, F. [2007] *Motion coordination with distributed information*, IEEE Control Systems Magazine, **27**(4), 75–88.

Meester, R. and Roy, R. [2008] *Continuum Percolation*, Cambridge University Press, ISBN 0521062500.

Mesbahi, M. [2005] *On state-dependent dynamic graphs and their controllability properties*, IEEE Transactions on Automatic Control, **50**(3), 387–392.

Mitchell, J. S. B. [1997] *Shortest paths and networks*, in *Handbook of Discrete and Computational Geometry*, J. E. Goodman and J. O'Rourke, editors, chapter 24, pages 445–466, CRC Press, ISBN 0849385245.

Okabe, A., Boots, B., Sugihara, K., and Chiu, S. N. [2000] *Spatial Tessellations: Concepts and Applications of Voronoi Diagrams*, second edition, Wiley Series in Probability and Statistics, John Wiley, ISBN 0471986356.

O'Rourke, J. [2000] *Computational Geometry in C*, Cambridge University Press, ISBN 0521649765.

Penrose, M. [2003] *Random Geometric Graphs*, Oxford Studies in Probability, Oxford University Press, ISBN 0198506260.

Preparata, F. P. and Shamos, M. I. [1993] *Computational Geometry: An Introduction*, Springer, ISBN 0387961313.

Radke, J. D. [1988] *On the shape of a set of points*, in *Computational morphology. A computational geometric approach to the analysis of form.*, G. T. Toussaint, editor, pages 105–136, North-Holland, ISBN 0-444-70467-1.

Robert, J.-M. and Toussaint, G. T. [1990] *Computational geometry and facility location*, in *Int. Conf. on Operations Research and Management Science*, pages 1–19, Manila, The Philippines.

Sack, J. R. and Urrutia, J., (editors) [2000] *Handbook of Computational Geometry*, North-Holland, ISBN 0444825371.

Santi, P. [2005] *Topology Control in Wireless Ad Hoc and Sensor Networks*, John Wiley, ISBN 0470094532.

Sibson, R. [1981] *A brief description of natural neighbour interpolation*, in *Interpreting Multivariate Data*, V. Barnett, editor, pages 21–36, John Wiley, ISBN 0471280399.

Tutuncu, R. H., Toh, K. C., and Todd, M. J. [2003] *Solving semidefinite-quadratic-linear programs using SDPT3*, Mathematical Programming, Series B, **95**, 189–217.

Whiteley, W. [1997] *Rigidity and scene analysis*, in *Handbook of Discrete and Computational Geometry*, J. E. Goodman and J. O'Rourke, editors, chapter 49, pages 893–916, CRC Press, ISBN 0849385245.

Subject Index

Symbol Index

$\mathcal{G}$	: proximity graph, 14
$\mathcal{G}_{\mathrm{D}}$	: Delaunay graph, 15
$\mathcal{G}_{\mathrm{EMST},\mathcal{G}}$	: Euclidean minimum spanning tree of $\mathcal{G}$, 16
$\mathcal{G}_{\mathrm{EMST}}$	: Euclidean minimum spanning tree of the complete graph, 16
$\mathcal{G}_{\mathrm{G}}$	: Gabriel graph, 16
$\mathcal{G}_{\mathrm{lc},\mathcal{G}}$	: locally cliqueless graph of $\mathcal{G}$, 20
$\mathcal{G}_{\mathrm{RN}}$	: relative neighborhood graph, 15
$\mathcal{G}_{\mathrm{cmplt}}$	: complete proximity graph, 14
$\mathcal{G}_{\mathrm{disk}}(r)$	: r-disk graph, 15
$\mathcal{G}_{\infty\text{-}\mathrm{disk}}(r)$	: r-∞-disk graph, 16
$\mathcal{G}_{\mathrm{LD}}(r)$	: r-limited Delaunay graph, 15
$\mathcal{G}_{\mathrm{vis},Q}$	: visibility graph in Q, 16
$\mathcal{G}_{\text{vis-disk},Q}$	: range-limited visibility graph in Q, 16
$i_{\mathbb{F}} : X^n \to \mathbb{F}(X)$	: natural immersion of X^n into $\mathbb{F}(X)$, 20
$\mathrm{IC}(S)$	: incenter of S, 10
$\mathrm{IR}(S)$	: inradius of S, 10
$\mathrm{kernel}(S)$	: visibility kernel set of S, 7
$\mathcal{N}_{\mathcal{G}}$	: set of neighbors map of $\mathcal{G}$, 17
$\mathrm{rco}(S; X)$	: relative convex hull of S in X, 9
$\mathrm{Ve}(Q)$	: vertices of Q, 7
$\mathrm{Vi}(p; S)$	: set of all points in S visible from p, 7
$\mathrm{Vi}_{\mathrm{disk}}(p; S)$	: set of all points in S within a distance r and visible from p, 7
$V_i(\mathcal{P})$	: Voronoi cell of p_i, 12
$V_{i,r}(\mathcal{P})$	: r-limited Voronoi cell of p_i, 12
$\mathcal{V}(\mathcal{P})$	: Voronoi partition generated by $\mathcal{P} = \{p_1, \ldots, p_n\}$, 12
$\mathcal{V}_r(\mathcal{P})$	: r-limited Voronoi partition generated by $\mathcal{P} = \{p_1, \ldots, p_n\}$, 12